Modelling Requirements for CFD Calculations of Spray Dyers

M. Sommerfeld

Mechanische Verfahrenstechnik
Zentrum für Ingenieurwissenschaften
Martin-Luther-Universität
Halle-Wittenberg
D-06099 Halle (Saale), Germany
www-mvt.iw.uni-halle.de

Jornadas em Escoamentos Multifásicos

Campinas, Brazil, March 23-27, 2015

Content of the Lecture

- Transport processes and physical phenomena in spray dryers
- Modelling requirements for numerical calculations of spray dryers
- Summary of Euler/Lagrange approach
- New droplet drying model
- Validation: single droplets and spray dryer
- Droplet/particle collision phenomena in spray dryers
- Stochastic inter-particle collision model
- Collisions of high-viscous droplets (experimental and modelling)
- Structure resolving particle agglomeration model
- Exemplary spray dryer calculations with agglomeration
- Conclusions and outlook

Introduction 1

☞ **Spray dryers are being used in many industrial areas (e.g. food, pharma, detergents and building) to convert a solution or suspension into a powder of defined properties.**

Injection of hot air with swirl

Suspension or solution

Atomisation
Droplet break-up
Droplet collisions

Droplet motion
Droplet drying

Particle collisions
Agglomeration

Air and fine particles
Cyclone and bag filter

Powder with defined properties

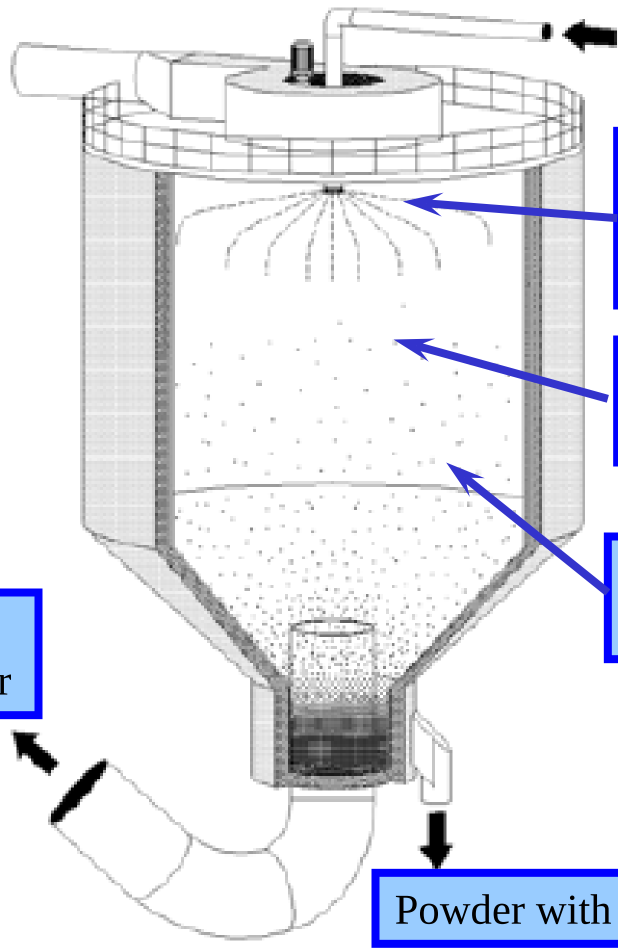

Recycling of fine powder

Collisions and agglomeration

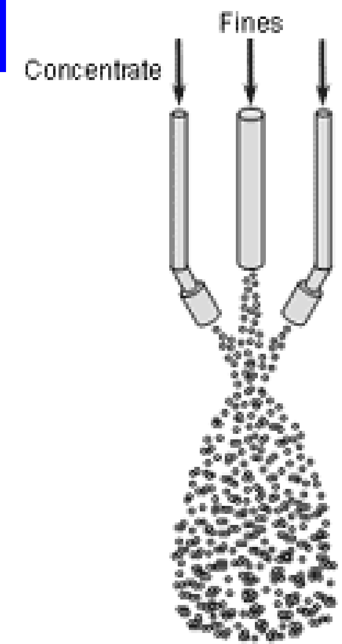

Introduction 2

- **A spray dryer is used for converting a solution or suspension into solid powder for further processing, transportation or commercial use.**
- **Quite often the main target is producing a powder of desired properties which has certain properties (particle design).**
- Up to now the design of spray dryers and the determination of the operational conditions are based on a try-and-error approach in pilot-scale experiments.
- This procedure is however not very satisfactory since it is time consuming and rather costly.

Brochure GEA Niro Spray Dryers

- Since about 20 years, however, numerical approaches based on CFD (computational fluid dynamics) are increasingly applied for dryer design and optimization.
- **Due to the importance of particle size distribution the Euler/Lagrange approach is beneficial for such simulations.**
- A thorough computational tool is however not existing due to the numerous elementary processes influencing powder production in a spray dryer.

Fletcher et al. Applied Mathematical Modelling 30 (2006) 1281–1292

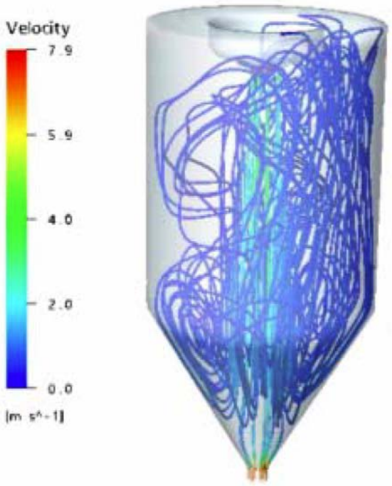

(a) zero swirl case

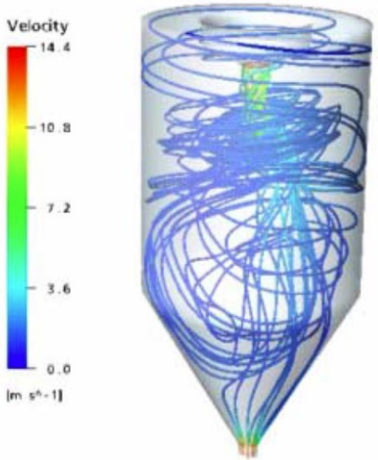

(c) 25° swirl angle case

Introduction 3

Fluid Flow Simulation ← **Two-Way Coupling** → **Particle Phase Simulation**

⇨ ***Grid generation***

⦿ ***URANS (unsteady Reynolds-averaged conservation equations)***

- ***Effect of particles on flow and turbulence***

⦿ ***LES (large-eddy simulations)***

- ***Modification of sub-grid-scale turbulence***

⇨ ***Gas phase properties (Vel, P, T, Species, ρ, μ)***

Atomisation model (droplet injection)

- Simple blob model
- Spatially resolved droplet size and velocity measurements

Secondary break-up of droplets

- Wave, Rayleigh-Taylor, TAB, ETAB/CAB (Tanner 2004)
- Comparison by Kumzerova et al (2007)

➔ Droplet tracking

- Relevant fluid forces (i.e. drag, lift, particle shape)
- Turbulence effect (isotropic, anisotropic turbulence)

➔➔ Droplet drying

- Change of solids content and droplet properties (μ and σ)
- Turbulence effects (instantaneous temperature field seen by the droplets)

➔➔ Droplet collisions

- Bouncing
- Coalescence
- Separation (formation of satellite droplets)

➔➔ Collisions of partially dried particles

- Partial or full penetration
- Modelling of agglomerate structure

Droplet/particle wall collisions

- Deposition or rebound collision (wall contamination)

Advantages of the *Euler-Lagrange approach* for spray dryer applications.

❖ Descriptive modelling of elementary processes

❖ Consideration of droplet/particle size distribution

Euler/Lagrange Approach 1

The **fluid flow** is calculated by solving the Reynolds-averaged conservation equations by accounting for two-way coupling (source terms).

Turbulence model: → **k-ε turbulence model**

- Conservation equations for: $\phi = 1, u, v, w, k, \varepsilon, Y, T$

$$\frac{\partial}{\partial x}(\rho u \phi) + \frac{\partial}{\partial y}(\rho v \phi) + \frac{\partial}{\partial z}(\rho w \phi) - \frac{\partial}{\partial x}\left(\Gamma \frac{\partial \phi}{\partial x}\right) - \frac{\partial}{\partial y}\left(\Gamma \frac{\partial \phi}{\partial y}\right) - \frac{\partial}{\partial z}\left(\Gamma \frac{\partial \phi}{\partial z}\right) = S_\phi + S_{\phi,p,m} + S_{\phi,p,ev}$$

The **Lagrangian approach** relies on the tracking of a large number of representative point-particles (parcels) through the flow field accounting for all relevant forces like: →

- drag force
- gravity/buoyancy
- slip/shear lift
- slip/rotation lift
- torque on the particle

+ models for small-scale phenomena

Particle properties and Source Terms result from ensemble averaging

Two-way coupling procedure with under-relaxation

In-house code FASTEST/Lag-3D

Euler/Lagrange Approach 2

Dispersed phase (particles):

$$\frac{d\vec{x}_p}{dt} = \vec{u}_p$$

Depending on the nature of the dispersed phase and the density ratio different relevant forces have to be used.

$$m_P \frac{d u_{P,i}}{d t} = \underbrace{\frac{3}{4}\frac{\rho}{\rho_P D_P} m_P C_D \left(u_i - u_{P,i}\right)\left|\vec{u} - \vec{u}_P\right|}_{❶} + \underbrace{\frac{\rho_F}{2}\frac{\pi}{4} D_p^2 C_{LS} D_P \left(\left(\vec{u}_F - \vec{u}_p\right)\times\vec{\omega}_F\right)}_{❷}$$

$$+ \underbrace{\frac{\rho_F}{2}\frac{\pi}{4} D_p^2 C_{LR} \left|\vec{u}_F - \vec{u}_P\right| \frac{\vec{\Omega}\times\left(\vec{u}_F - \vec{u}_P\right)}{\left|\vec{\Omega}\right|}}_{❸} + \underbrace{m_P g_i \left(1 - \frac{\rho}{\rho_P}\right)}_{❹} + \underbrace{F_i}_{❺}$$

- ❶ drag force
- ❷ slip-shear lift
- ❸ slip-rotation lift
- ❹ gravity/ buoyancy
- ❺ other forces, e.g. electrostatic

Rotation:

$$I_p \frac{d\vec{\omega}_p}{dt} = \frac{\rho_F}{2}\left(\frac{D_p}{2}\right)^5 C_R \left|\vec{\Omega}\right|\cdot\vec{\Omega}$$

- **The instantaneous fluid velocity is generated by a single-step Langevin model.**

$$u^f_{i,n+1} = R_{P,i}\left(\Delta t, \Delta r\right) u^f_{i,n} + \sigma_i \sqrt{1 - R^2_{P,i}\left(\Delta t, \Delta r\right)}\, \xi_i$$

New droplet drying model with validation for a spray dryer

Droplet Drying Model 1

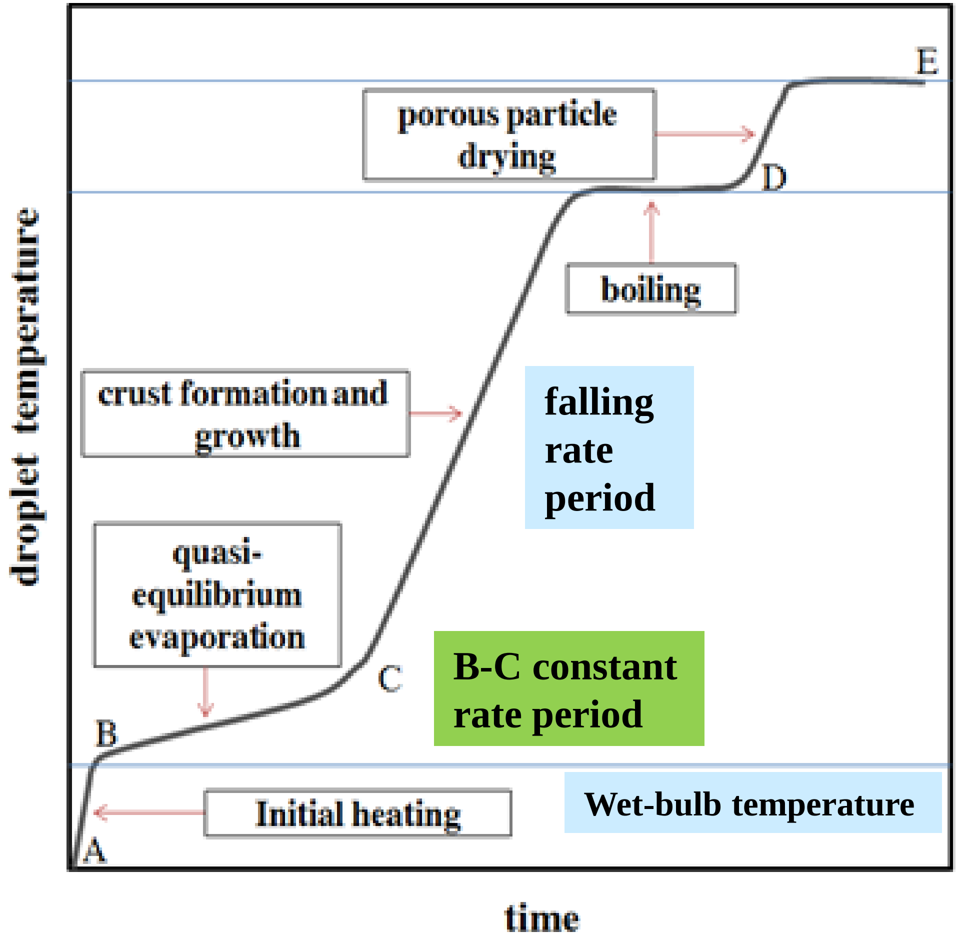

Drying stages of a spherical solution or suspension droplet

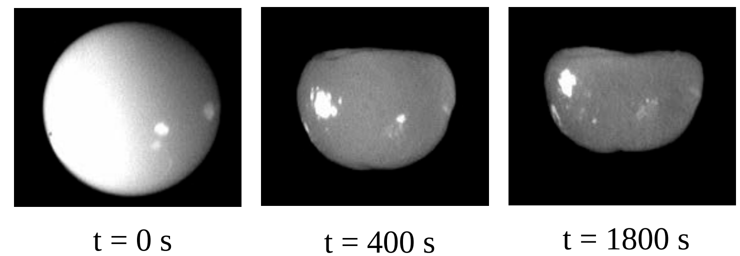

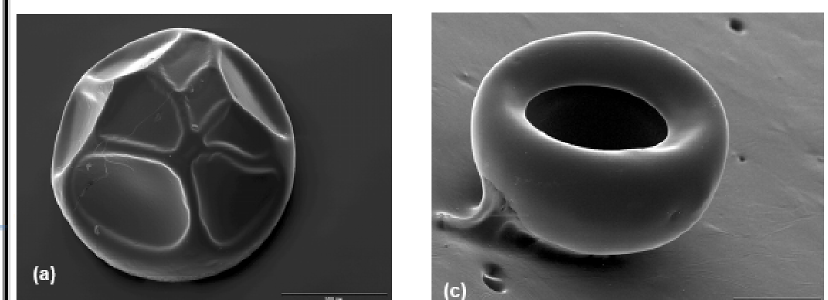

Two possible paths of droplet drying

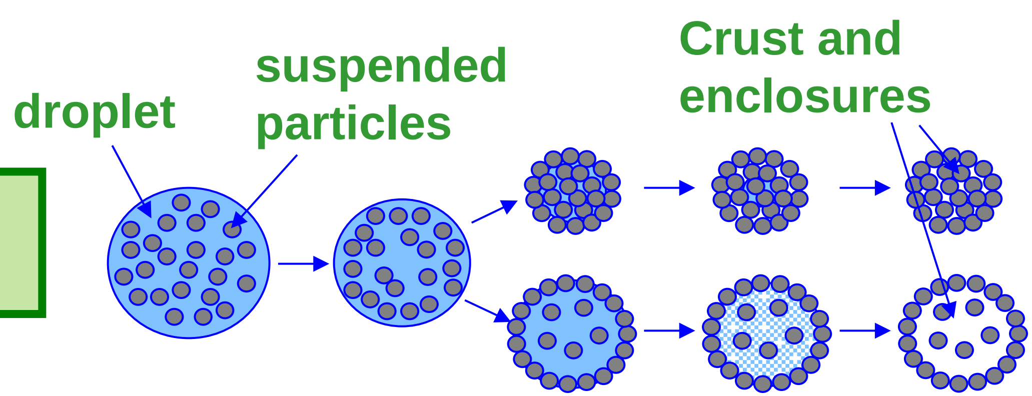

Droplet Drying Model 2

❖ A Mechanistic model is used to describe the four stages of droplet drying (Darvan & Sommerfeld, IDS 2014)

➢ **Stage A-B**, initial heat-up period (sensible heating)

- T_S → equilibrium temperature (wet bulb temperature)
- Temperature distribution inside the droplet:

$$\frac{dT}{dt} = \frac{\alpha}{r^2} \cdot \frac{\partial}{\partial r}\left(r^2 \cdot \frac{\partial T}{\partial r}\right)$$

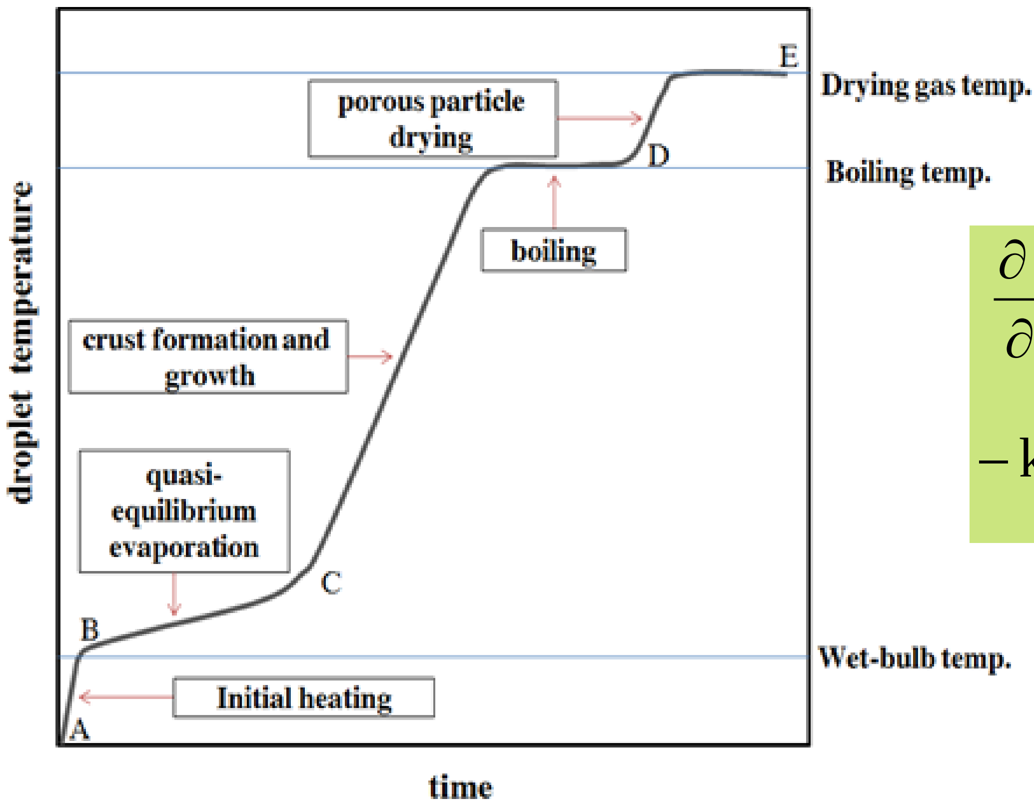

$$\frac{\partial T}{\partial r} = 0 \qquad \text{at:} \quad r = 0$$

$$-k\,\frac{\partial T}{\partial r} = h\left(T_s - T_\infty\right) \qquad \text{at:} \quad r = R$$

α: droplet thermal diffusivity
k: thermal conductivity
h: air heat transfer coefficient

Droplet Drying Model 3

- **Stage B-C, quasi-equilibrium evaporation (like liquid droplets), change of droplet temperature (constant rate period):**
  - **T_S is slightly higher than the bulb temperature**
  - **Constant further increase due to rising solids concentration**
  - **Change of droplet temperature:**

$$2\,\pi\,R\,Nu\,\lambda_{air}\left(T_\infty - T_s\right) = m\,C_v\,\frac{dT}{dr} + L\,\frac{dm}{dt}$$

$$Nu = 2 + 0.6\,Re^{0.5}\,Pr^{0.33}$$

  - **Rate of evaporation by diffusion of vapour through the boundary layer around the droplet (gas phase resistance) depending on vapour concentration γ [kg/m^3]:**

$$\frac{dm}{dt} = 2\,\pi\,R\,Sh\,D_{air}\left(\gamma_s - \gamma_\infty\right)$$

$$Sh = 2 + 0.6\,Re^{0.5}\,Sc^{0.33}$$

- **Stage C-D, crust formation and boiling (falling rate period):**
  - Surface concentration C_S reaches the saturation C_{sat}
  - Crust formation due to crystallisation
  - droplet shrinkage is stopped
  - Two regions: dry outer crust and inner wet core (fully saturated)
  - Discretisation of core and crust region
  - Interface tracking
  - Calculation of temperature distribution (crust and core region)

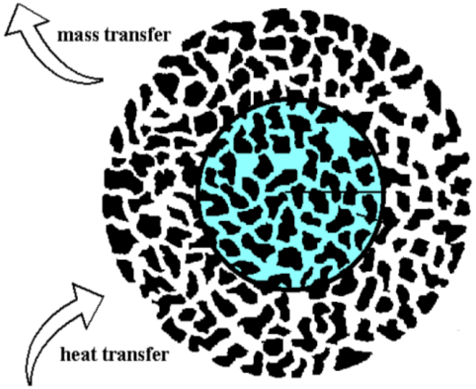

$$\frac{dT}{dt} = \frac{r}{R_{int}} \frac{dR_{int}}{dt} \frac{\partial T}{\partial r} + \frac{\alpha}{r^2} \cdot \frac{\partial}{\partial r}\left(r^2 \cdot \frac{\partial T}{\partial r}\right)$$

$$\frac{\partial T}{\partial r} = 0 \qquad \text{at: } r = 0$$

$$-k \frac{\partial T}{\partial r} = h\left(T_s - T_\infty\right) \qquad \text{at: } r = R$$

$$T = T_{wb} \qquad \text{at: } r = R_{int}$$

α: droplet thermal diffusivity
k: thermal conductivity
h: air heat transfer coefficient

Droplet Drying Model 5

- **The heat balance at the interface (R_{int}) is used to track the interface in time (depending on thermal conductivity of crust and core):**

$$\left(\omega_0 - \omega_b\right) L \, \rho_{av} \frac{d R_{int}}{d t} = -\left(k_{crust} \frac{\partial T}{\partial r}\bigg|_{r=R,int} \right) - \left(k_{core} \frac{\partial T}{\partial r}\bigg|_{r=R,int} \right)$$

- **Vapour diffusion through boundary layer around liquid core and through the crust:**

$$\frac{dm}{dt} = \frac{2 \pi \left(\gamma_s - \gamma_\infty\right)}{\dfrac{1}{R_{cri} \, Sh \, D_{air}} + \dfrac{\delta}{2 D_{crust} \, R_{cri} \left(R_{cri} - \delta\right)}}$$

- **Solids concentration distribution within the droplet (diffusion):**

$$\frac{\partial C}{\partial r} = \frac{1}{r^2} \frac{\partial}{\partial r} \left(r^2 D_{AB} \frac{\partial C}{\partial r} \right)$$

Internal diffusion of solids for skimmed milk

$$D_{AB} = \left\{ \frac{\left(38.912 + 323.39 \, \omega_A\right)}{\left(1 + 15.8 \, \omega_A\right)} - \frac{\Delta H}{R} \left(\frac{1}{T} - \frac{1}{303} \right) \right\}$$

ω_A: moisture content droplet
ΔH: activation energy diffusion

- **Stage D-E, porous particle drying:**
  - **Bounded liquid is evaporated with decreasing rate**
  - **Temperature asymptotically approaches surrounding gas temperature**
  - **Temperature distribution inside the dried particle estimated by taking into account only the crust thermo-physical properties:**

$$\frac{\partial T}{\partial t} = \frac{\alpha}{r^2} \cdot \frac{d}{dr}\left(r^2 \cdot \frac{dT}{dr} \right)$$

$$\frac{dT}{dr} = 0 \qquad \text{at:} \quad r = 0$$

$$-k\frac{dT}{dr} = h\left(T_s - T_\infty\right) \qquad \text{at:} \quad r = R$$

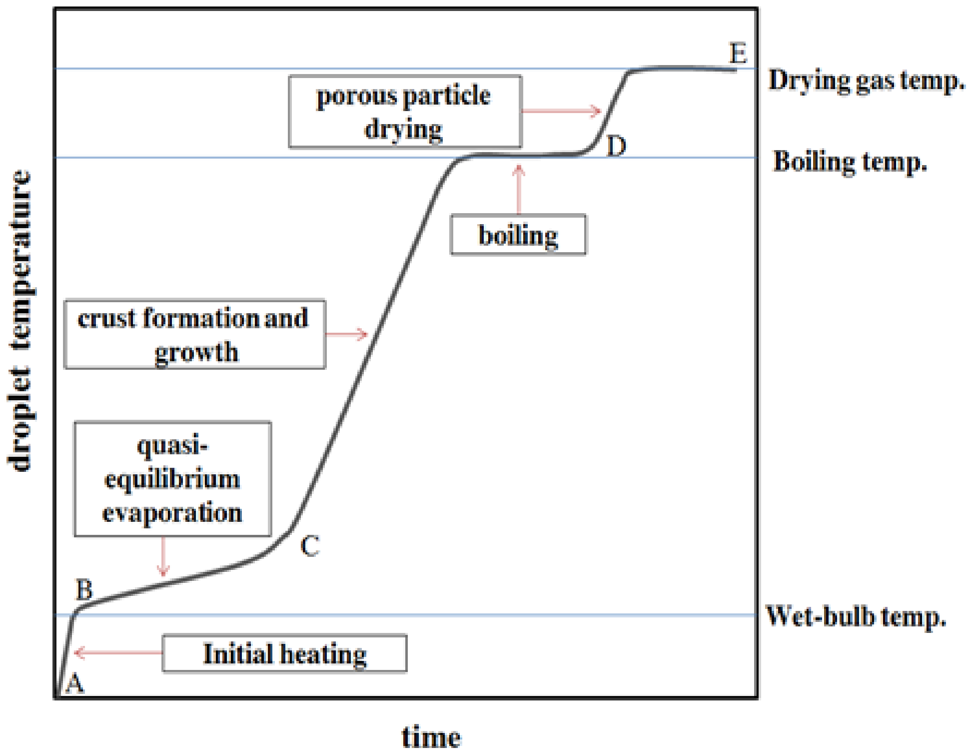

Droplet Drying Model 7

➢ **Comparison of the new drying model with experiments and „classical models“**

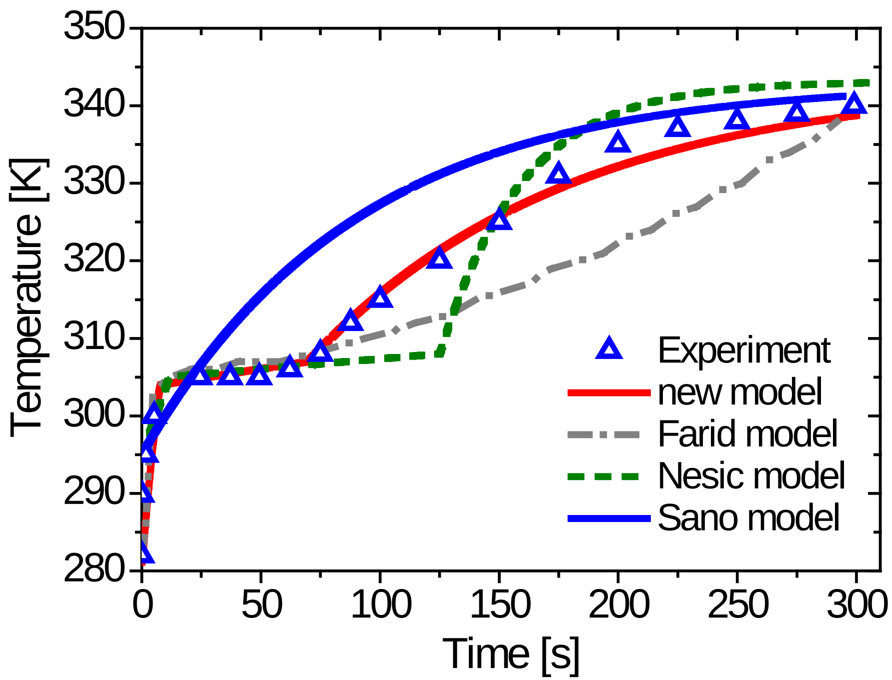

Experiments for skim milk (solids 20% mass) by Chen et al. (1999):
V_{air} = 1.0 m/s
T_{air} = 343 K
$T_{drop,0}$ = 282 K
D_0 = 1.9 mm

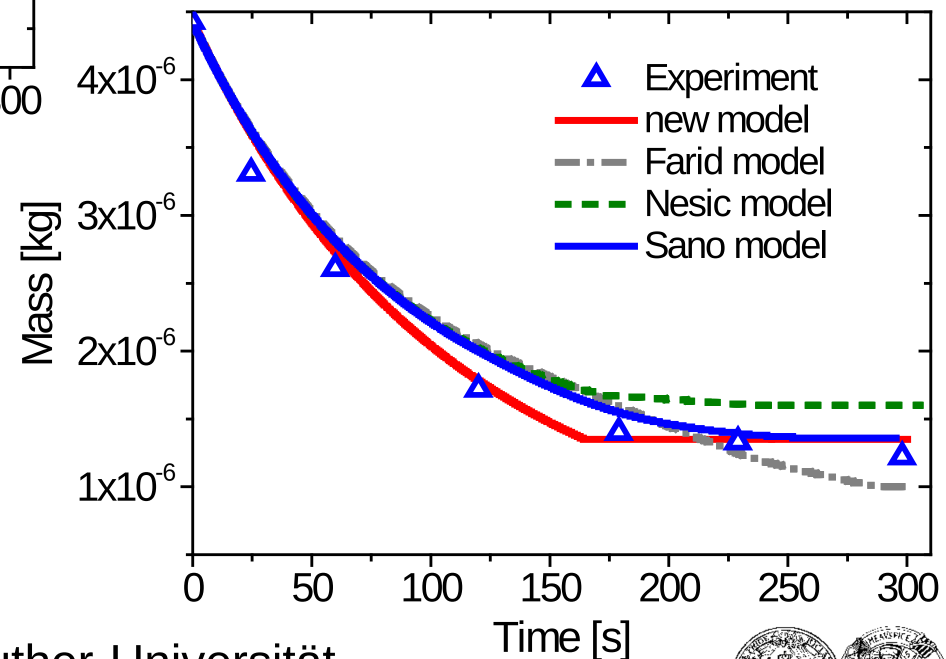

Droplet Drying Model 8

- **Comparison of the new drying model with experiments:**

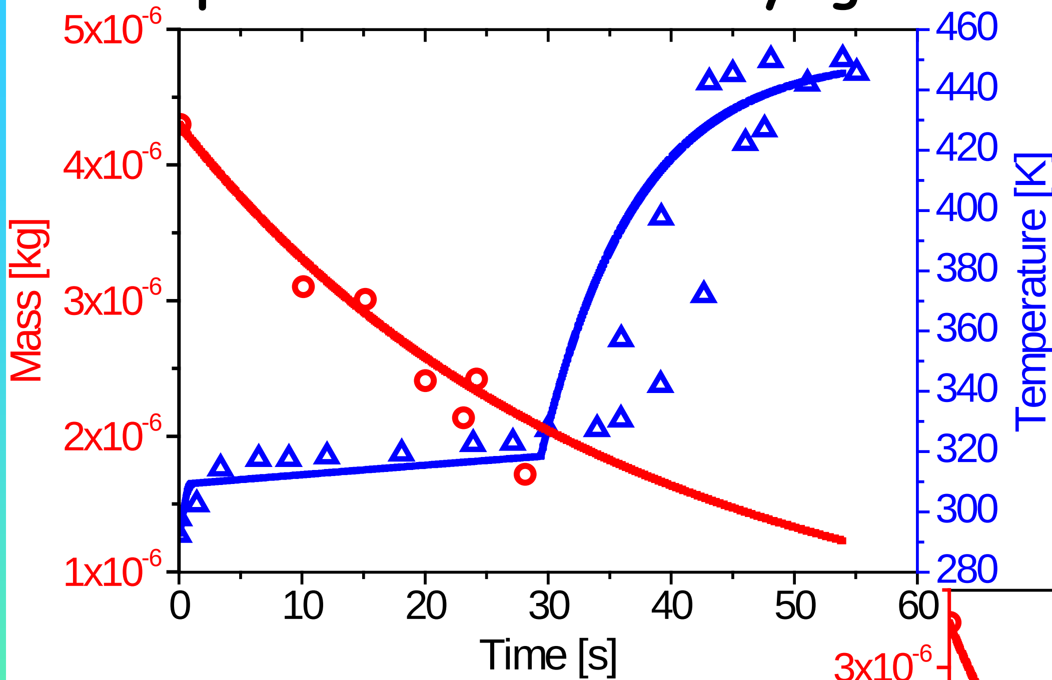

Colloidal silica, 30 % mass
(Nesic & Vodnik 1991)
V_{air} = 1.4 m/s
T_{air} = 451 K
$T_{drop,0}$ = 293 K
D_0 = 2 mm

Sodium sulphate in water,
14 % mass
(Nesic & Vodnik 1991)
V_{air} = 1.0 m/s
T_{air} = 383 K
$T_{drop,0}$ = 297 K
D_0 = 1.85 mm

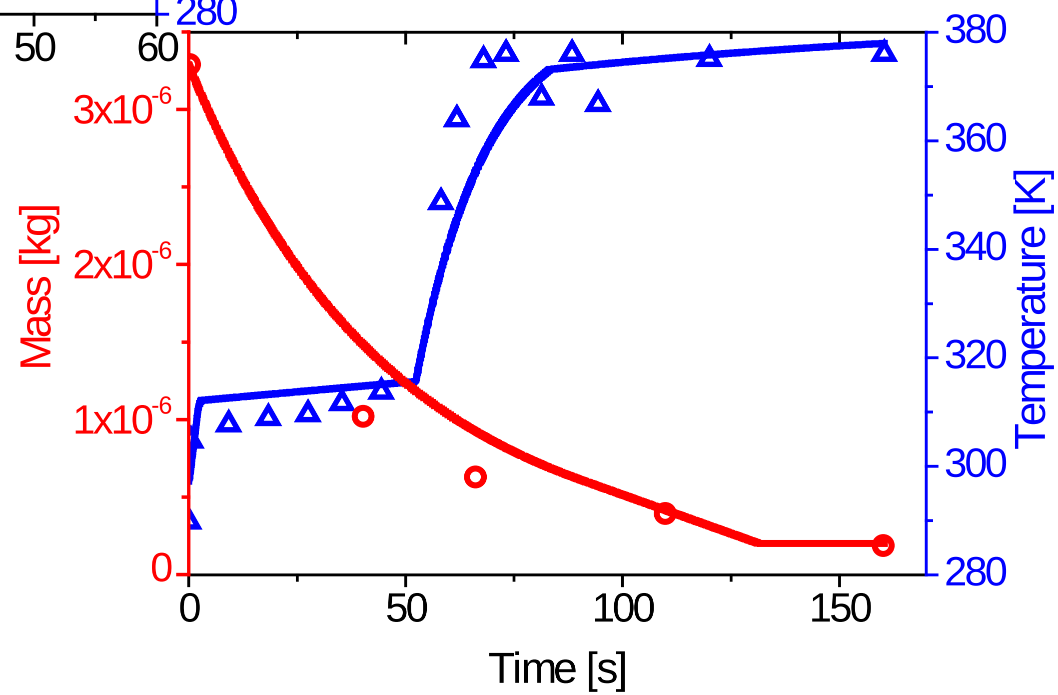

Droplet Drying Model 9

➢ **Radial distribution of mass and temperature within the droplet**

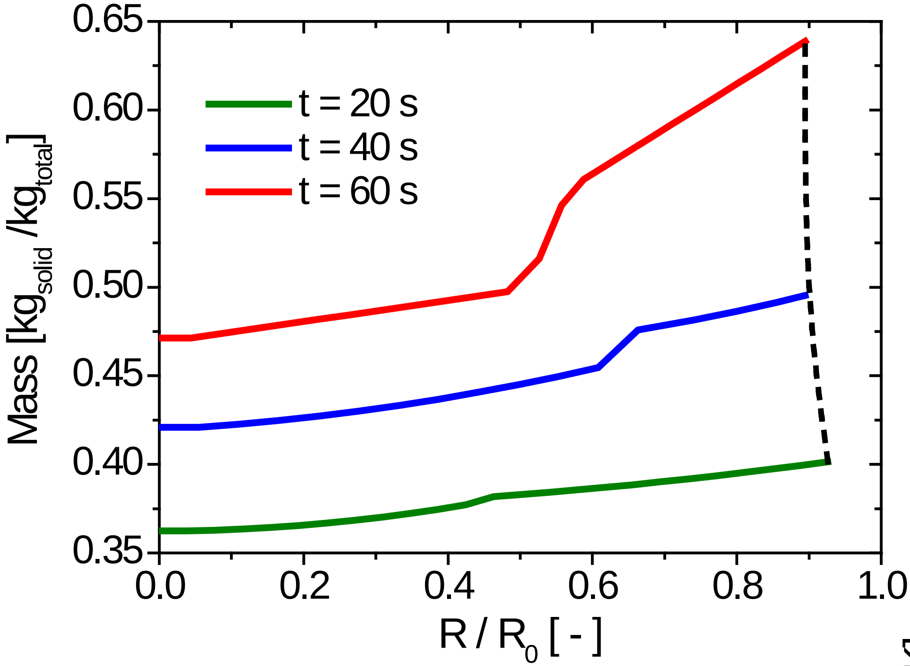

Experiments for skim milk (solids 30% mass) by Sano & Keey (1985)
V_{air} = 1.0 m/s
T_{air} = 423 K
$T_{drop,0}$ = 301 K
D_0 = 1.9 mm

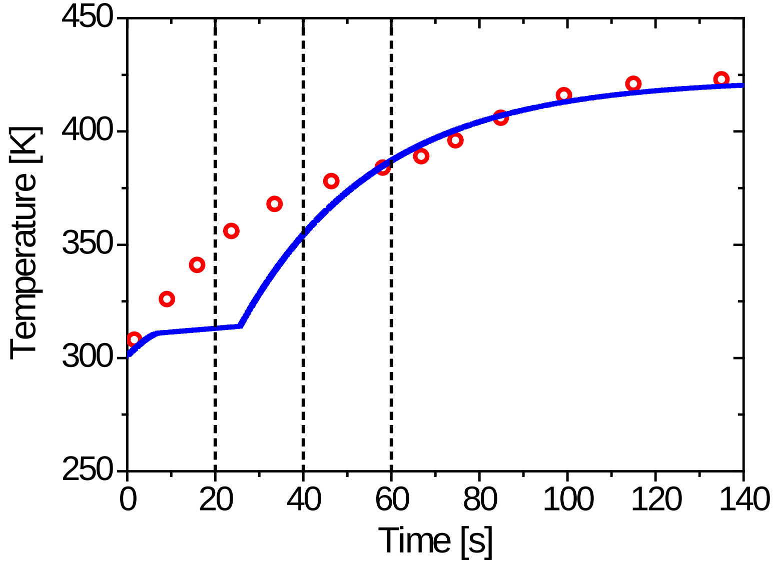

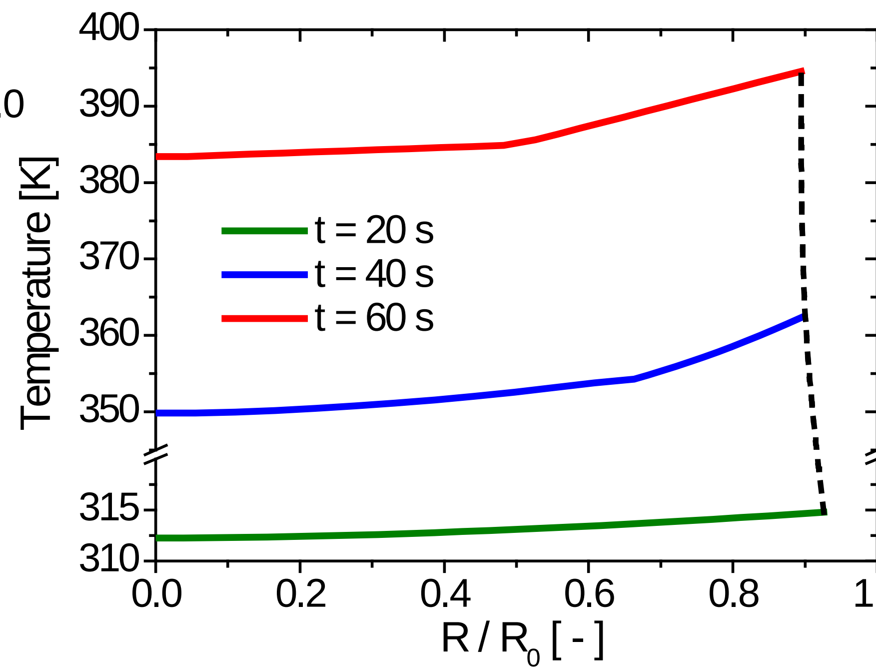

14:50

Spray Dryer 1

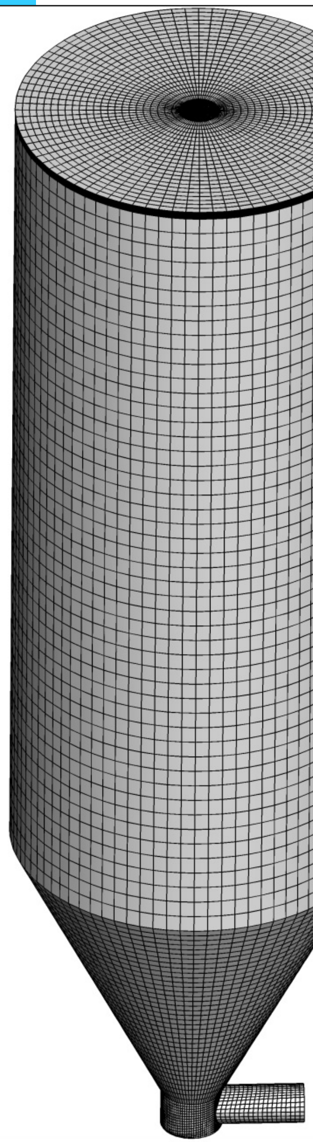

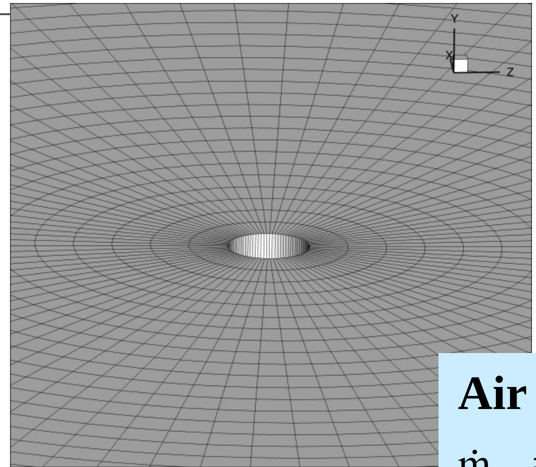

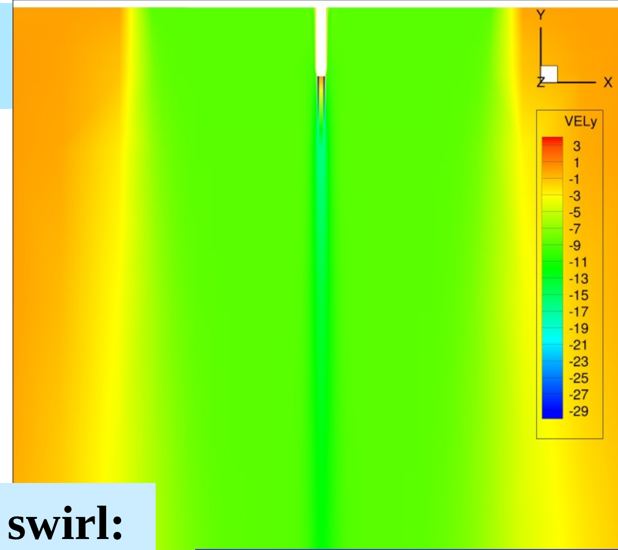

Air flow, no swirl:

$\dot{m}_{air}$ = 226.8 kg/h

T_{air} = 444 K

U_{ax} = 8.87 m/s

U_{tan} = 0.0 m/s

Dryer geometry:

H = 2980 mm

H_{cyl} = 2120 mm

D = 900 mm

D_{out} = 95 mm

Annular Air Inlet

D_o = 100 mm

R_i = 3.05 mm

Two-Fluid Nozzle:

Spray angle $\beta = 9^o$

$D_{nozzle,air,o}$ = 3.05 mm

$D_{nozzle,air,i}$ = 1.73 mm

H_{nozzle} = 200 mm

Whey Based

Solution: 30 mass-% solids

ρ_{drop} = 1002 kg/m^3

$\dot{m}_{solution}$ = 7.31 kg/h

$T_{solution}$ = 293 K

$U_{air, av}$ = 29.2 m/s

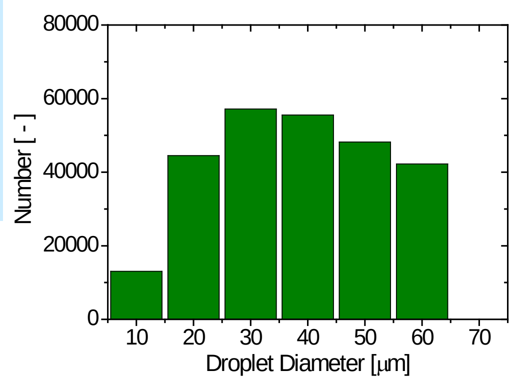

718,706 control volumes

Martin-Luther-Universität Halle-Wittenberg

Spray Dryer 2

➢ **Comparison of present calculations with results obtained with Fluent**

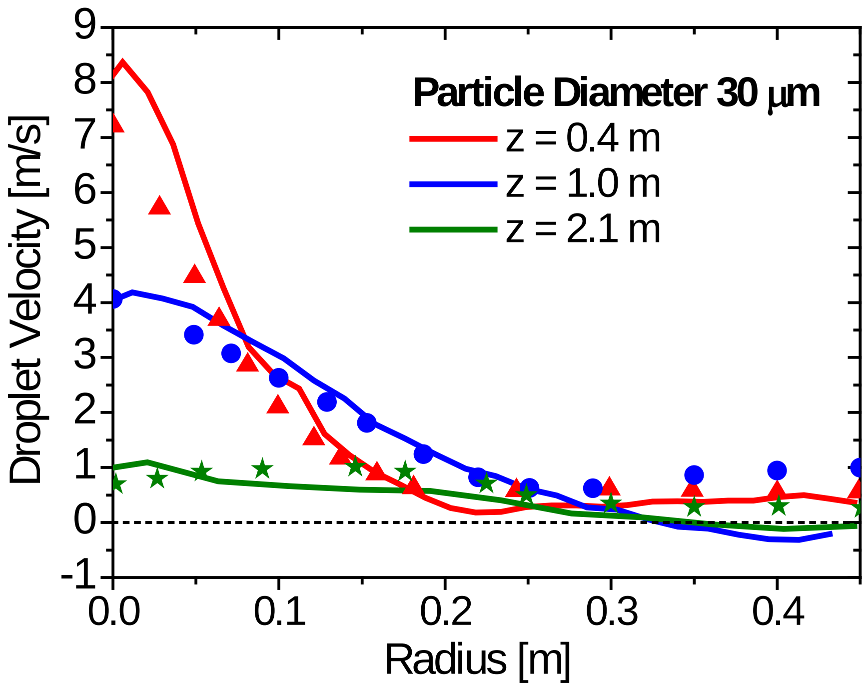

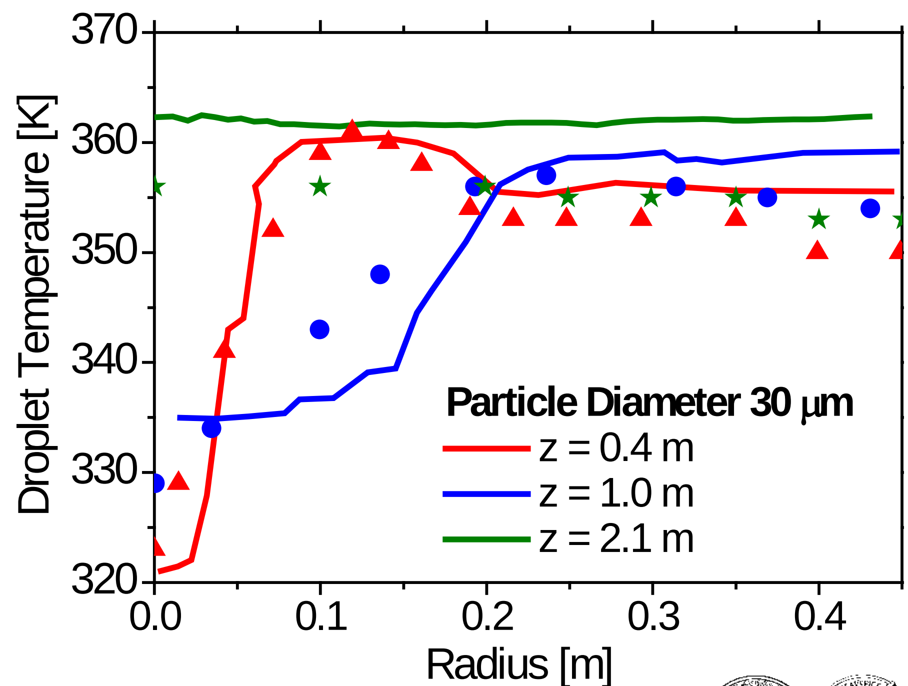

Droplet and particle collisions in spray dryer
stochastic inter-particle collision model
experiments for viscous droplets

Inter-Particle Collisions in Spray Dryers

Properties of droplets injected into a spray dryer (i.e. viscosity and surface tension) are strongly changing along their way through the dryer caused by drying of solution and suspension droplets (increasing solids content).

Collisions of droplets/particles with different drying state

Surface tension dominated droplets
- Vicinity of atomiser

Viscosity dominated droplets
- Middle region of dryer

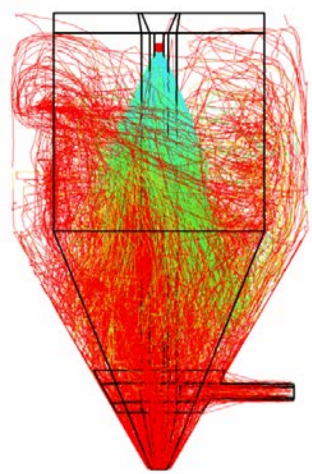

Droplets and solid particles
- Penetration
- Agglomerate formation
- Particle coating

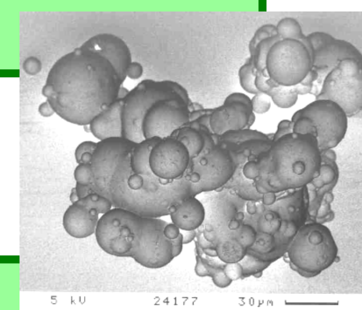

Solid particles (low moisture content)
- Agglomeration
- van der Waals forces

Martin-Luther-Universität
Halle-Wittenberg

Stochastic Inter-Particle Collision Model (Sommerfeld 2001)

- **In the trajectory calculation of the considered particle a fictitious collision partner is generated for each time step.**
- **The properties of the fictitious particle are sampled from local distribution functions and correlations with the particle size.**

⇨ particle diameter
⇨ particle velocities
⇨ particle temperature
⇨ solids content

- **In sampling the fictitious particle velocity fluctuation the correlation of the fluctuating velocity is respected (LES of Simonin):**

$$u'_{fict,i} = R(\tau_P, T_L)\, u'_{real,i} + \sigma_i \sqrt{1 - R(\tau_P, T_L)^2}\; \xi_n$$

$$R(\tau_p, T_L) = \exp\left(-0.55 \left(\frac{\tau_p}{T_L} \right)^{0.4} \right)$$

- **Calculation of collision probability between the considered particle and the fictitious particle:**

$$P = f_c\, \Delta t = \frac{\pi}{4} (D_{P1} + D_{P2})^2 \left| \vec{u}_{P1} - \vec{u}_{P2} \right| n_P\, \Delta t$$

- **A collision occurs when a random number in the range [0 - 1] becomes smaller than the collision probability.**

Stochastic Inter-Particle Collision Model 2

- The collision process is calculated in a co-ordinate system where the fictitious particle is stationary.

$$L = \sqrt{Y^2 + Z^2} \qquad \text{with:} \quad L \le 1$$

$$\phi = \arcsin(L)$$

$$0 < \Psi < 2\,\pi$$

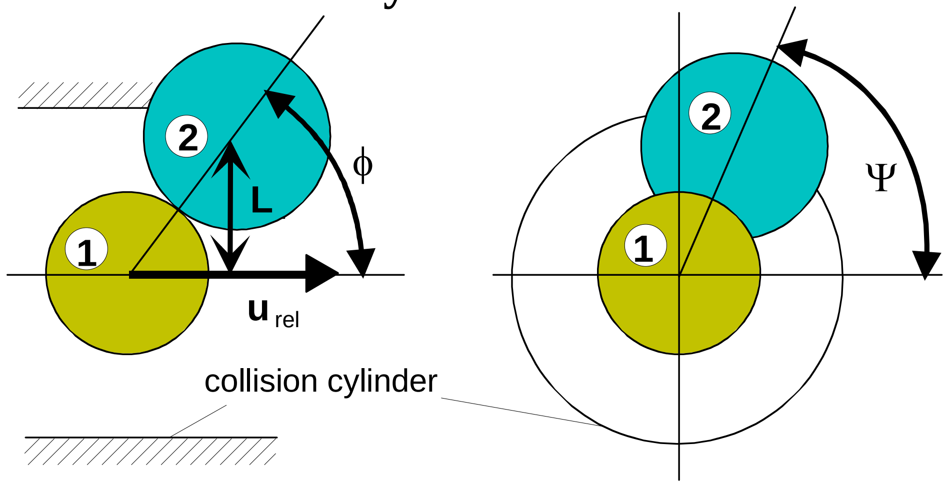

- Consideration of impact probability (small and large particles):

$$\eta = \left(\frac{2\,Y_c}{(D_K + d_p)}\right)^2 = \left(\frac{\Psi_i}{\Psi_i + a}\right)^b$$

$$\Psi_i = \frac{\rho_p \left|\vec{u}_{p1} - \vec{u}_{p2}\right| d_p^2}{18\,\mu\,D_K}$$

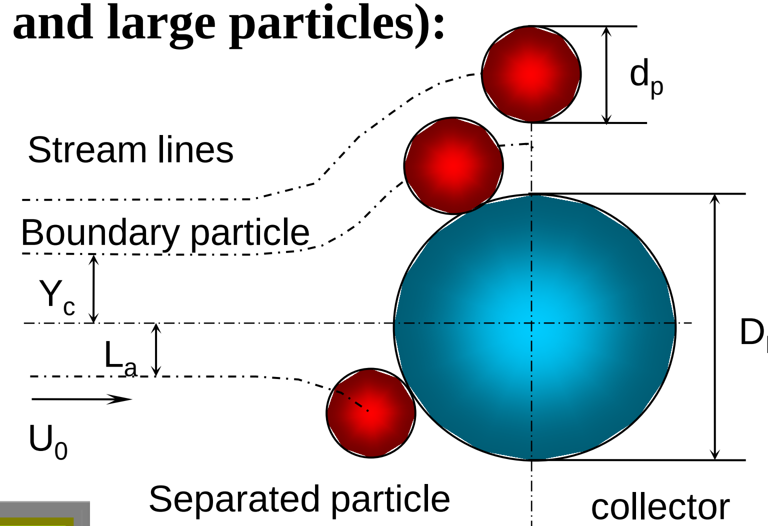

Collision occurs if: $L_a \le Y_C$

Stochastic Inter-Particle Collision Model 3

- **In the case of rebound the new velocities of the considered particle are calculated by solving the momentum equations for an oblique collision in connection with Coulombs law of friction.**

$$u'_{P1} = u_{P1}\left(1 - \frac{1+e}{1+m_{P1}/m_{P2}}\right)$$

Sliding collision

$$v'_{P1} = v_{P1}\left(1 - \mu\left(1+e\right)\frac{u_{P1}}{v_{P1}}\frac{1}{1+m_{P1}/m_{P2}}\right)$$

Non-sliding collision

$$\frac{v_{P1}}{u_{P1}} < \frac{7}{2}\mu\left(1-e\right)$$

$$v'_{P1} = v_{P1}\left(1 - \frac{7/2}{1+m_{P1}/m_{P2}}\right)$$

- **Re-transformation of the new particle velocities in the laboratory frame of reference.**
- **Particle rotation is not considered in agglomeration studies, due to the complex momentum exchange for structured agglomerates.**

Droplet Collision Modelling 1

☞ **The outcome of a droplet collision depends on numerous parameters, namely, the kinetic properties and the thermo-physical properties of gas and droplets.**

- ➲ Droplet velocities
- ➲ Droplet diameter ratio
- ➲ Impact angle

- ➲ Droplet liquid (density and viscosity)
- ➲ Surface tension
- ➲ Type of gas phase
- ➲ Gas phase pressure and temperature

☞ **Governing non-dimensional parameters for the collision process:**

$$We_C = \frac{\rho_l \, D_S \, \vec{U}_{rel}^2}{\sigma_l}$$

$$B = \frac{2\,b}{D_S + D_L}$$

$$\Delta = \frac{D_S}{D_L}$$

$$Oh_C = \frac{\mu_l}{\sqrt{\rho_l \, \sigma_l \, D_S}}$$

$$\phi = \arcsin(B)$$

S: small
L: large

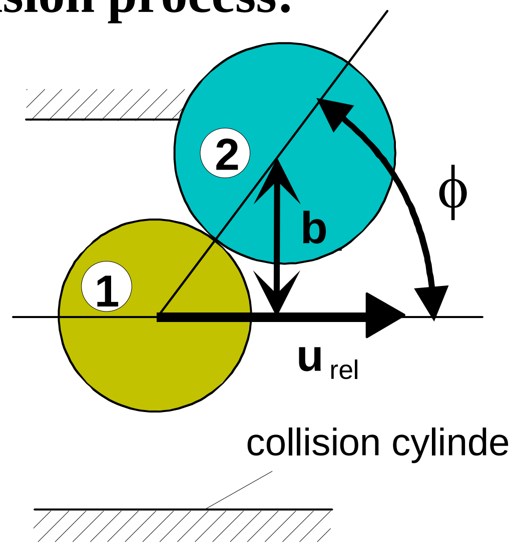

☞ **The different collision scenarios are generally summarised in a phase diagram, i.e. $B = f(We_C)$**

☞ **Due to the large number of relevant properties a unique solution for the collision regimes was not introduced so far !!!**

Droplet Collision Modelling 2

- Determination of the outcome of droplet collision based on B = f(We)

- **Calculation of post-collision droplet sizes and velocities**

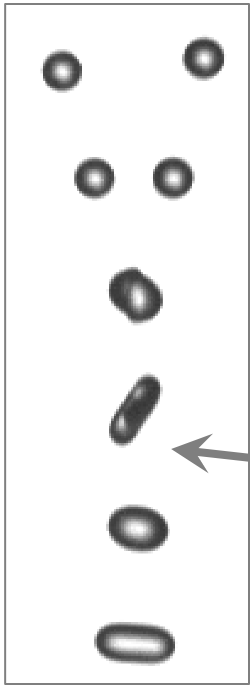

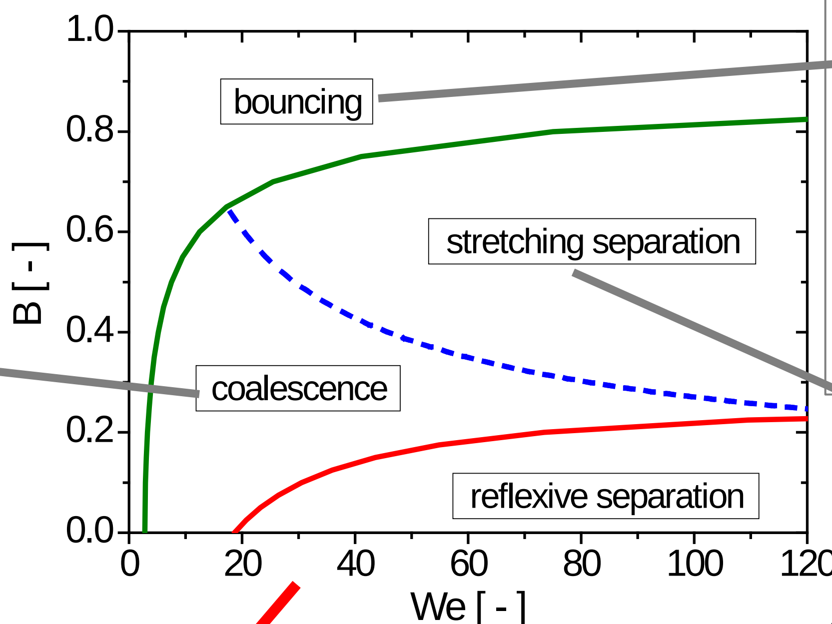

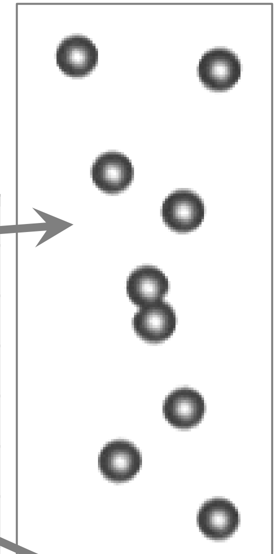

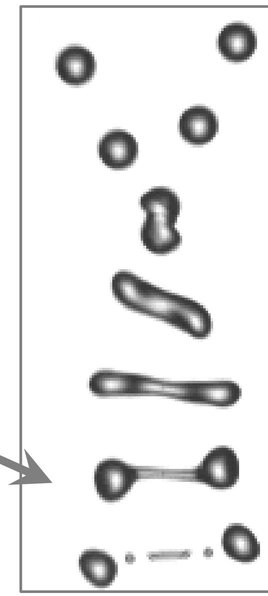

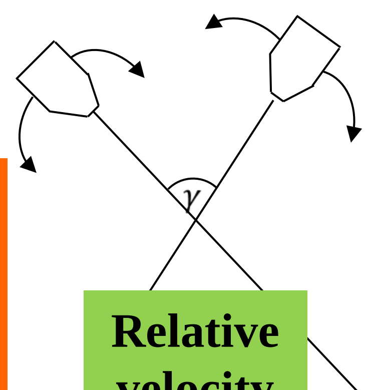

Not universally applicable → experiments to generalise the effect of viscosity

Relative velocity

substances (PVP K30, K17, Saccharose, series of alcohols, FVA 1 reference oil

Water for Validation

Kuschel & Sommerfeld
Exp. in Fluids, 2013

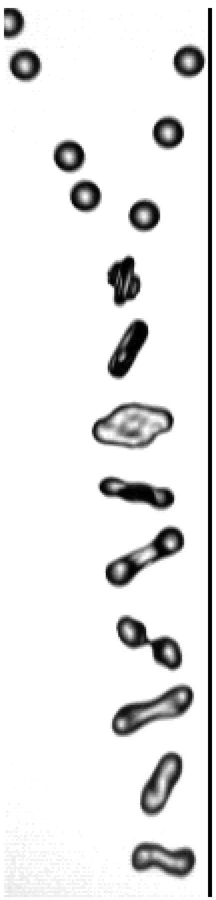

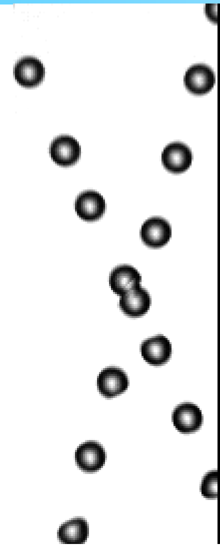

Images for We ~ 30

$$B = \frac{C_a}{We_d^{1/2}}\left[1 + C_b \frac{\mu_l}{\sigma_l}\left(\frac{\rho_l D_d}{\sigma_l}\right)^{1/2}\right]$$

$C_a = 2.33$ and $C_b = 0.41$

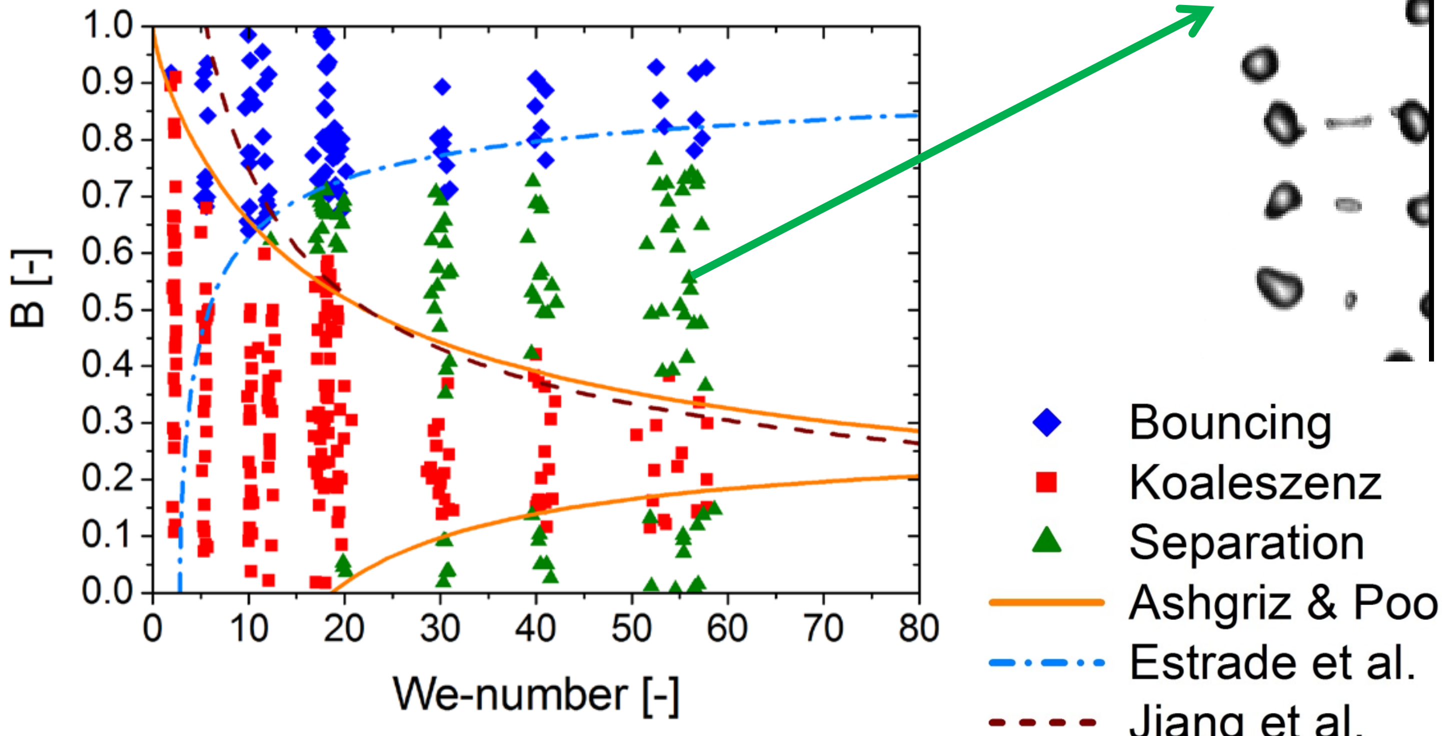

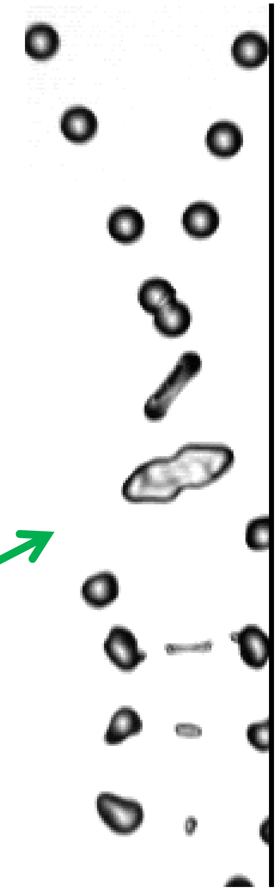

PVP K30 – 25 Ma%

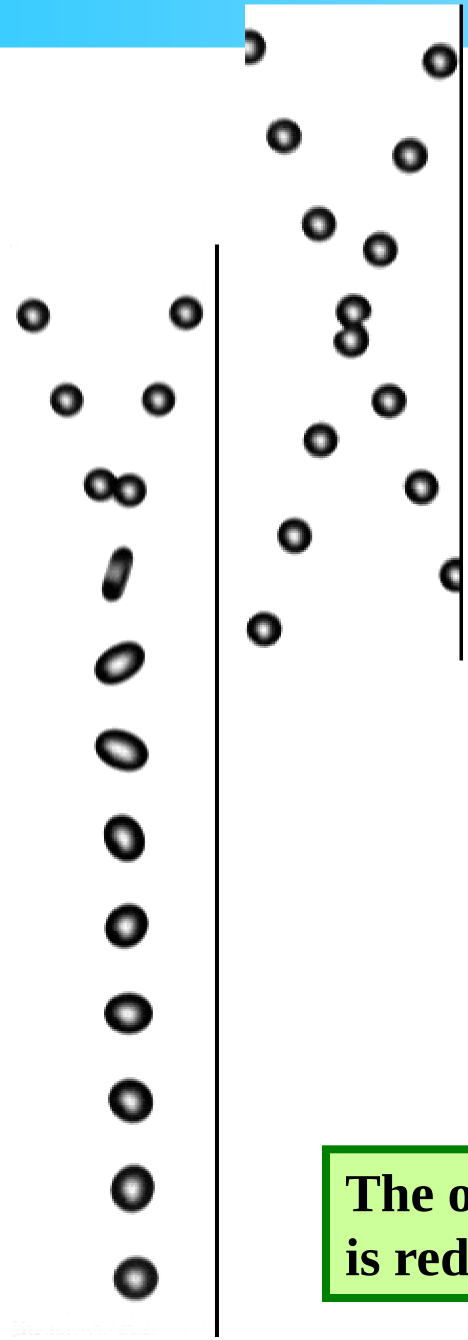

PVP K30: 25 Ma%, η = 60.0 mP s
Images for We ~ 30

C_a =2.3378 and C_b =0.24

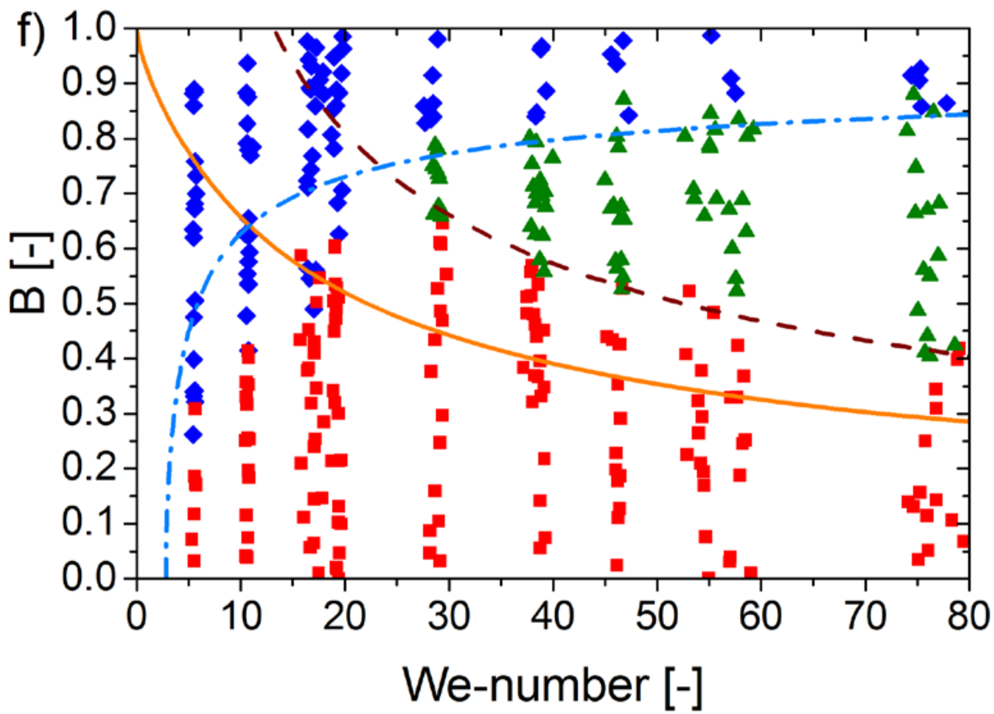

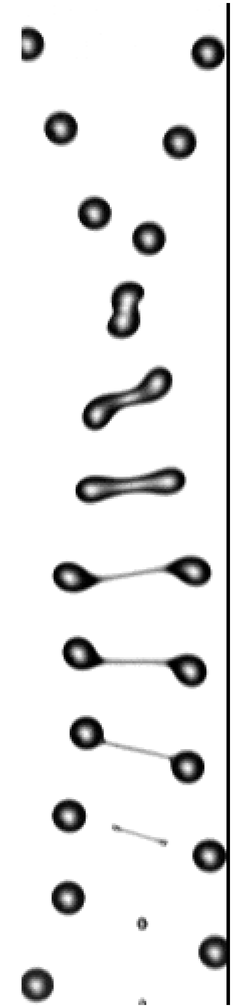

The oscillation of the droplets after coalescence is reduced with increasing dynamic viscosity

Modelling - Characteristic Points

- **Extraction of characteristic Triple Points (bouncing, coalescence and stretching separation collapse in one region) from the measurements for all substances**
- **The crossing point shows a clear dependence on viscosity (solids content)**

➡ ***Development of a maximum or minimum for u_{rel} and B, respectively***

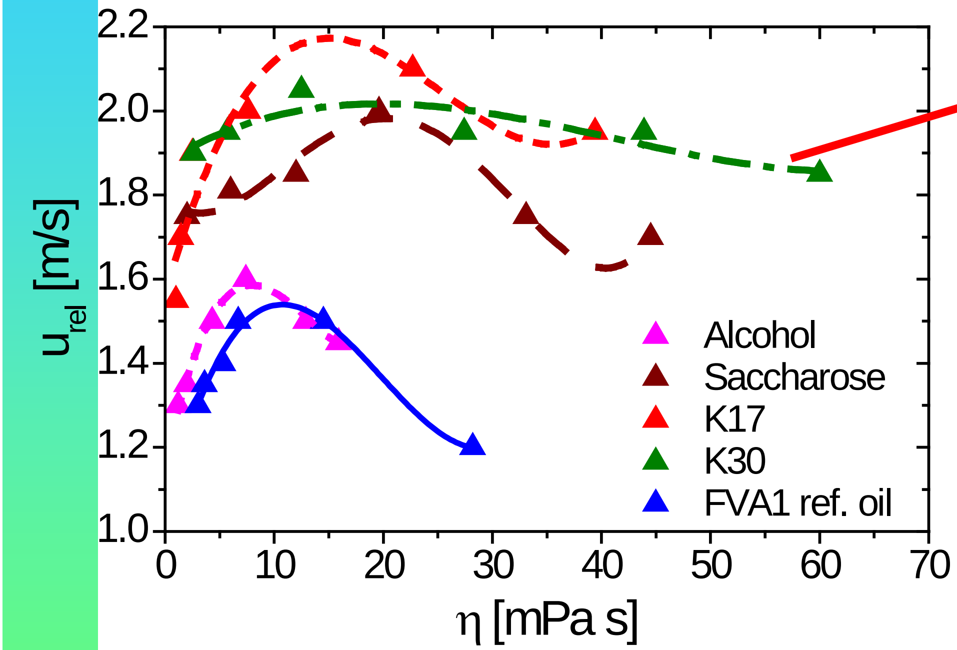

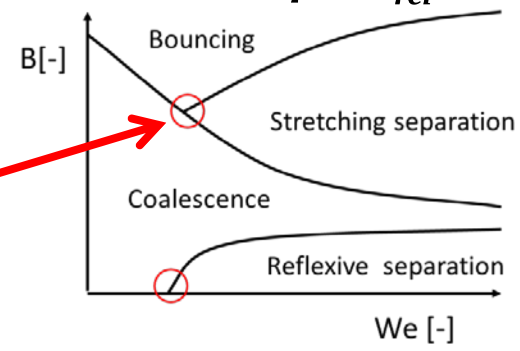

Sommerfeld & Kuschel ICMF Korea, 2013

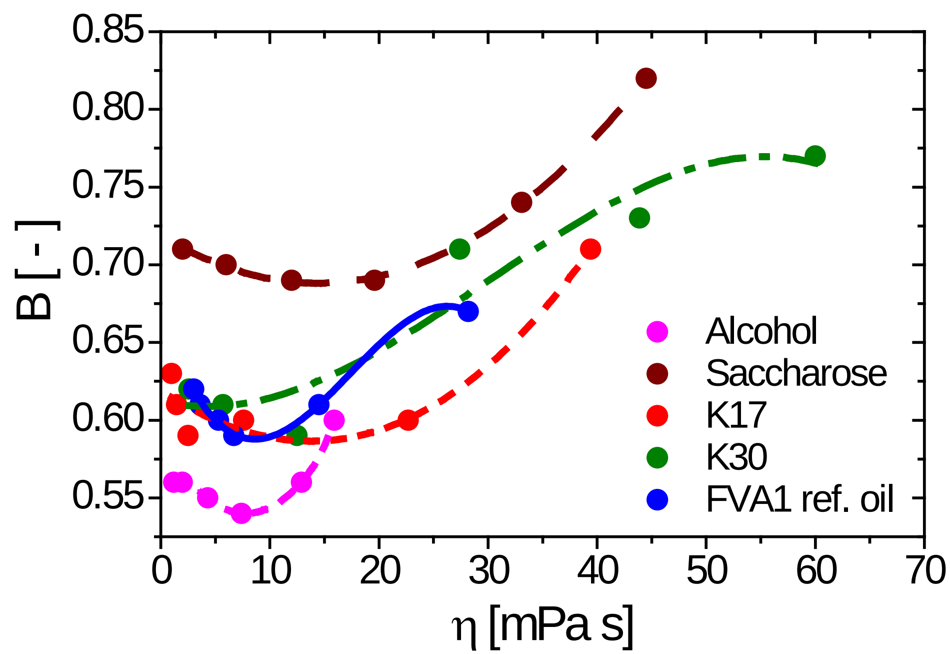

maximum/minimum location at:

$$u_{relax} = \frac{\sigma_l}{\mu_l} = 3.47\ m/s$$

Modelling Onset of Stretching Separation

➢ **Summary of Triple Point location for all systems**

⇨ Onset of stretching separation:

$$Re = \frac{K^2}{2} Ca^{-\sqrt{1-\frac{1}{e^2}}} \rightarrow We_C$$

K=6.9451*

Resulting from a theory on maximum of information entropy for competing processes, i.e. interaction of flow structures with the mean flow

$K^3 = 335$ → We for bubble break-up

$K^4 = 2326$ → critical Re for laminar-turbulent pipe flow

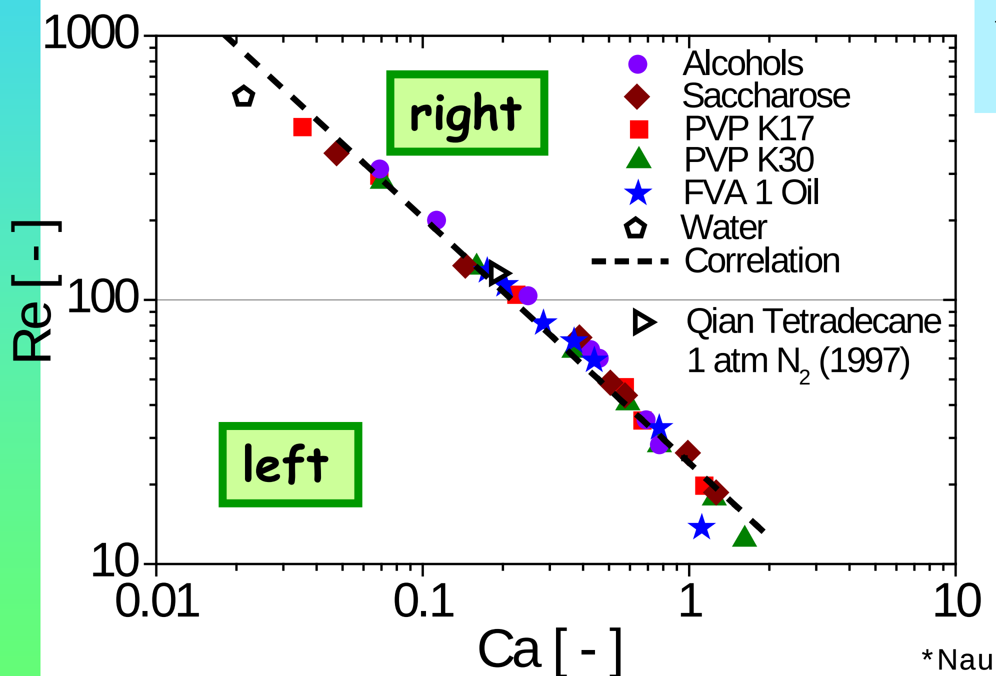

$$Re = \frac{\rho_l \, D_S \, U_{rel}}{\mu_l}$$

sliding of two fluid surfaces

$$Ca = \frac{\mu_l}{\sigma_l} U_{rel} = \frac{U_{rel}}{u_{relax}}$$

*Naue, G. and Bärwolff, G.: „Transportprozesse in Fluiden“, Deutscher Verlag für Grundstoff-Industrie, Leipzig, 1992.

Modelling Onset of Stretching Separation

➢ **Adaptation of the model of Jiang et al. (1992) to match triple**

$$B = \frac{C_a}{We^{1/2}} \left[1 + C_b \frac{\mu_l}{\sigma_l} \left(\frac{\rho_l D_d}{\sigma_l} \right)^{1/2} \right]$$

⇨ Optimal set of parameters for the Jiang model is a function of normalised relaxation velocity (here $u^*_{relax} = (\sigma/\mu)^* = 3.47$ m/s)

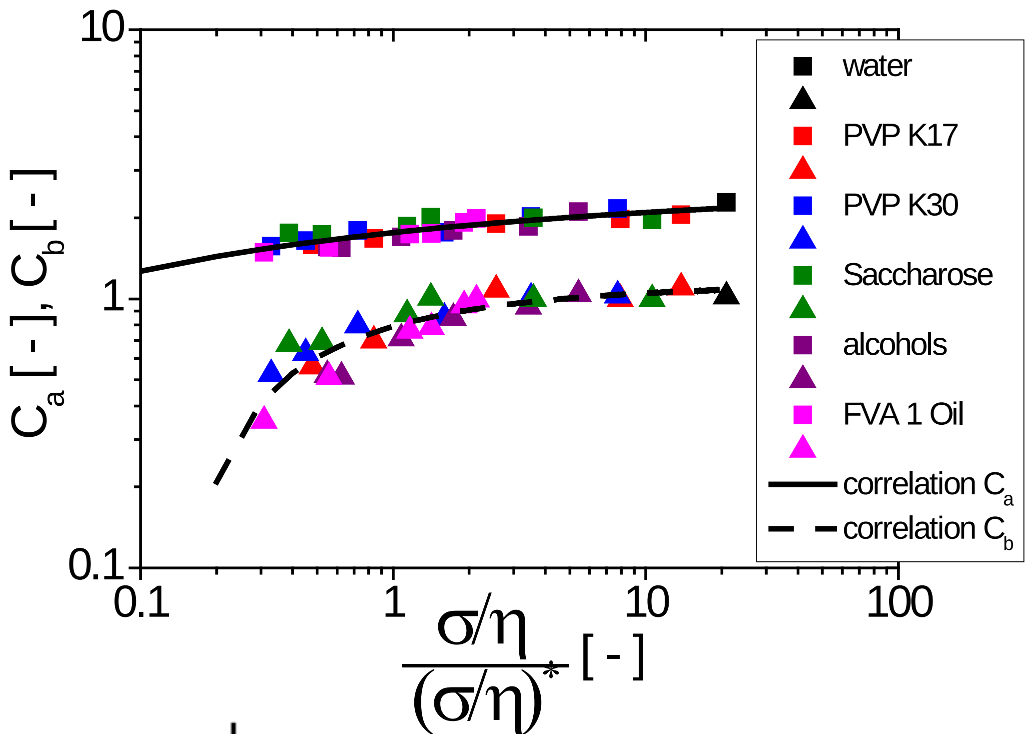

$$C_a = 2.762 - \left(\frac{u_{relax}}{u^*_{relax}} \right)^{-0.175}$$

$$C_b = 1.134 - 0.345 \left(\frac{u_{relax}}{u^*_{relax}} \right)^{-0.613}$$

$$\left(\frac{u_{relax}}{u^*_{relax}} \right) = \left(\frac{\sigma/\eta}{(\sigma/\eta)^*} \right)$$

Modelling - Onset of Reflexive Separation

➢ **Critical We for the beginning of reflexive separation (at B = 0)**

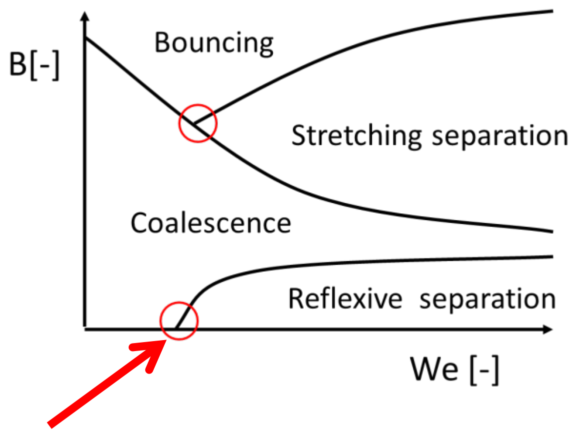

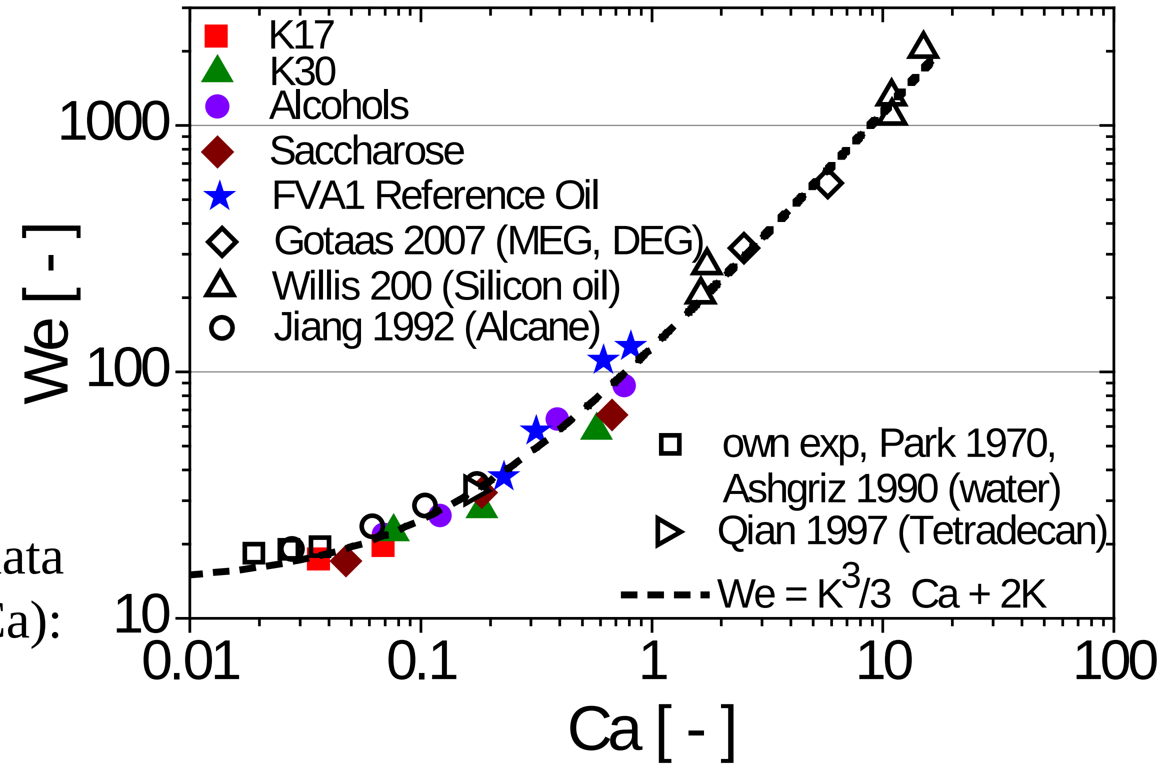

⇨ A correlation for all data can be found for We = f(Ca):

$$We = \frac{K^3}{3} Ca + 2K$$

K=6.9451 **Deformation of the droplets**

⇨ Modifying the model of Ashgriz and Poo to match critical We_{crit}:

$$We = We_{crit} + 3\left[7\left(1+\Delta^3\right)^{2/3} - 4\left(1+\Delta^2\right)\right]\frac{\Delta\left(1+\Delta^3\right)^2}{\Delta^6\,\eta_S + \eta_L}$$

Models Versus Experiments 1

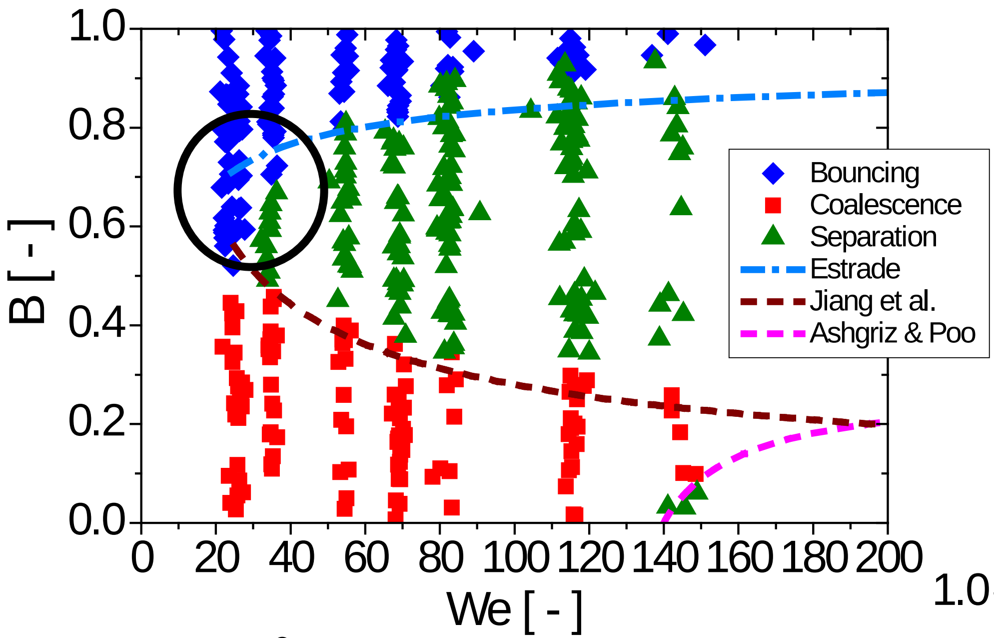

- The model of Ashgriz and Poo combined with the correlation for **reflexive separation** predicts the shift of the regime correctly

FVA 1, 60°
η = 6.7 mPa s

PVP K30, 15 %
η = 12.5 mPa s

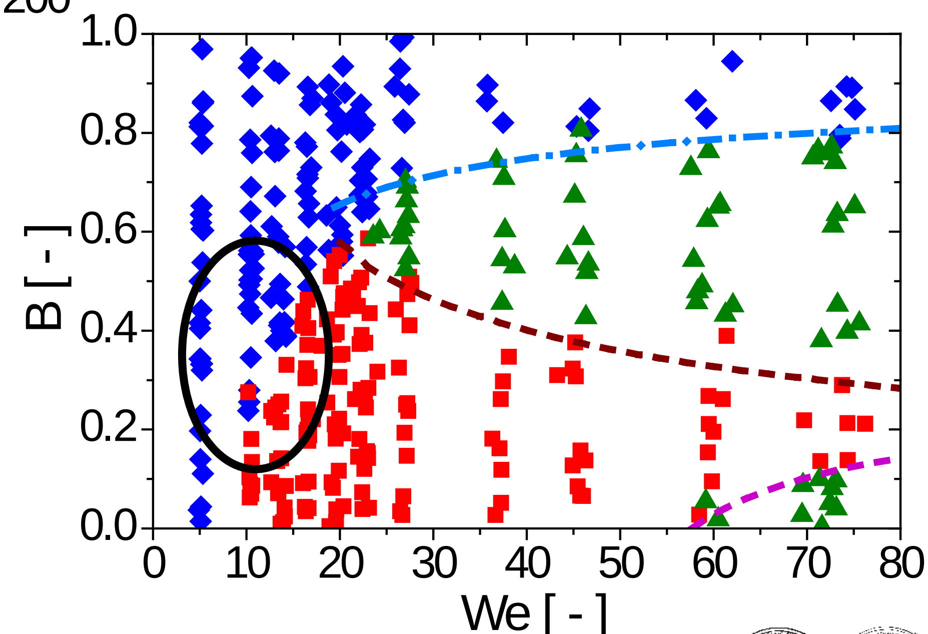

- The adapted model of Estrade et al. is reasonably good for higher We but shows systematic deviations for lower We

Models Versus Experiments 2

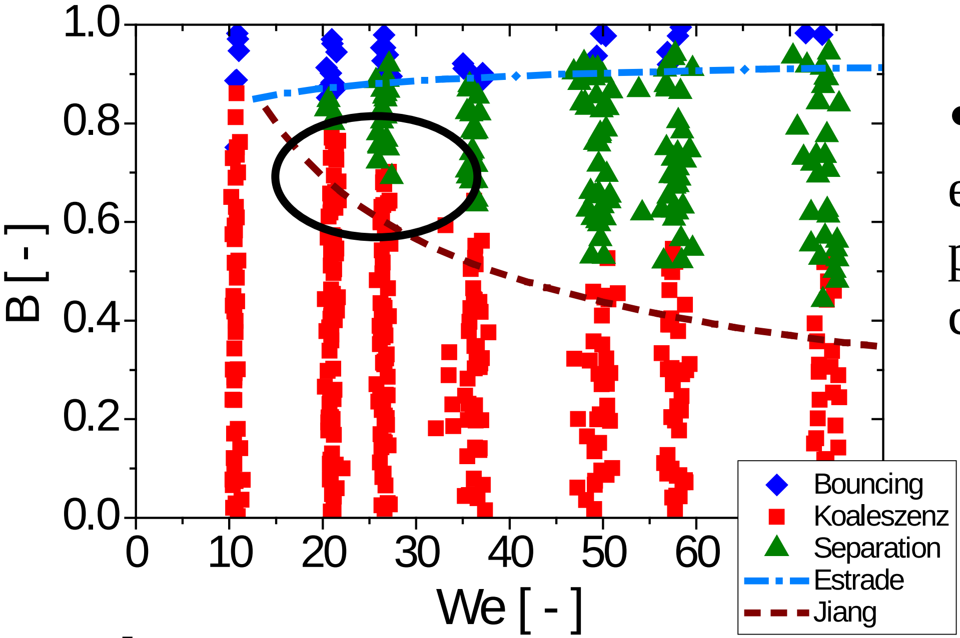

Saccharose 60 %
η = 57.3 mPa s

- For most of the substances the extended Jiang et al. model correctly predicts the boundary between coalescence and stretching separation

PVP K30, 25 %
η = 60 mPa s

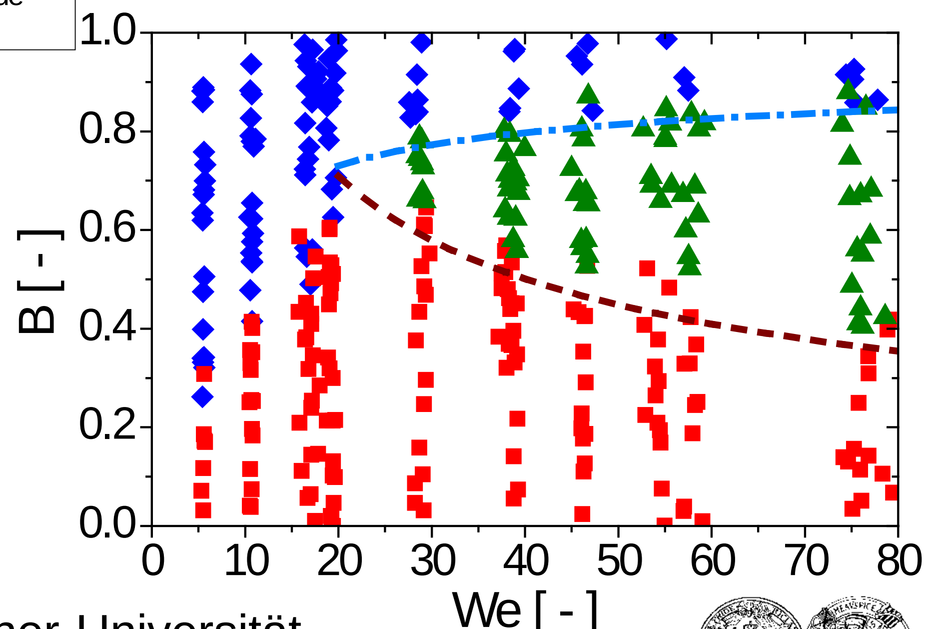

- Further studies are necessary for developing a general model for lower boundary of bouncing valid for the entire range of We

New structure agglomeration model with preliminary validation for a spray dryer

Agglomeration Model for Solid Particles

Sommerfeld & Stübing
ETMM 9, 2012

Agglomeration models

Point-particle assumption

Simple agglomeration model

Volume equivalent sphere

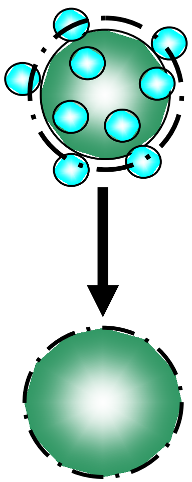

- Number of primary particles
- Penetration depth

Sequential agglomeration model

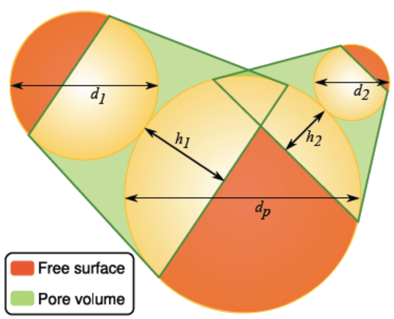

- Number of primary particles
- Hull volume/diameter
- Porosity of hull
- Contact forces

Agglomerate structure model

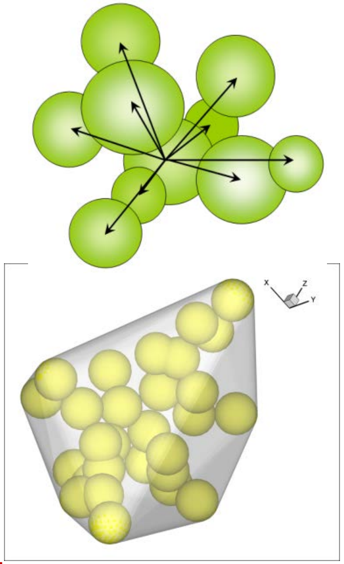

Location vectors
Convex hull

$$\varepsilon = 1 - \frac{V_{Part}}{V_{Hull}}$$

- Agglomerate structure
- Effective surface area
- Volume of convex hull
- Porosity of the agglomerate

Agglomerate Structure Model 1

☞ **In order to obtain more detailed information on the agglomerate structure, location vectors for all primary particles in the agglomerate with respect to a reference particle are stored.**

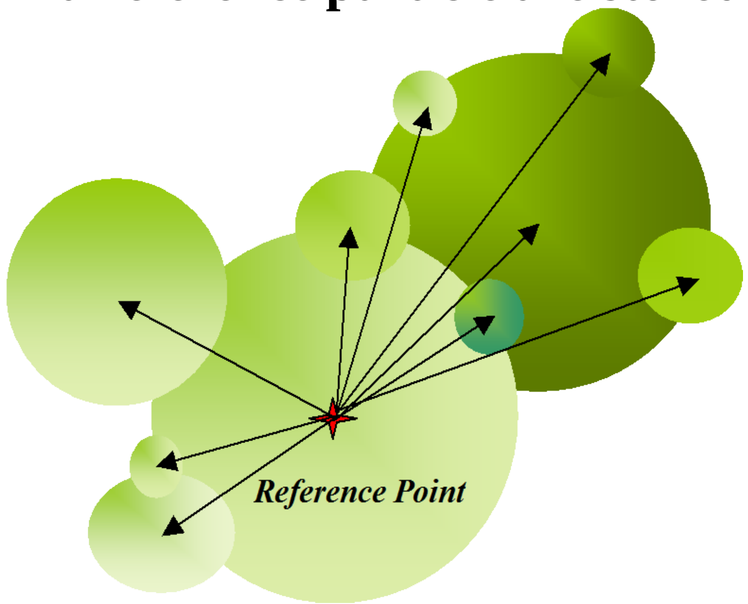

The agglomerate structure is stored in a linked list

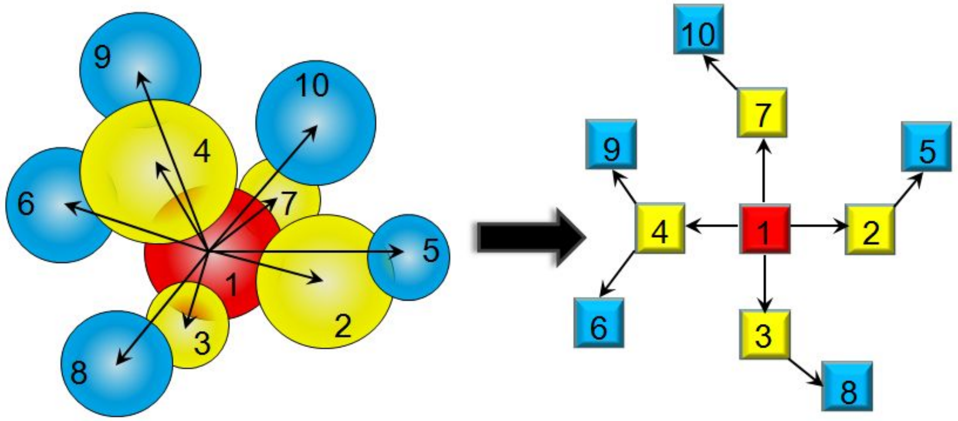

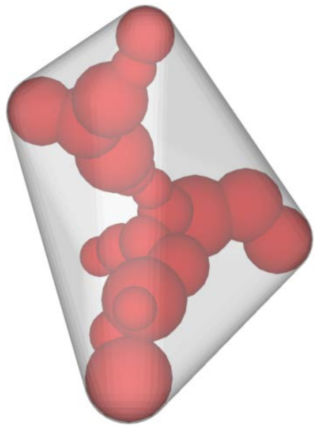

The agglomerate is still treated as point-particle !!!

Most important agglomerate properties

- **Porosity of the agglomerate (convex hull)**
- **Effective surface area**
- **Agglomerate structure; Shape indicators**

☞ Assumptions for the stochastic collision model with respect to structure modelling

- Agglomerates can only collide with primary particles (number concentration of the resulting agglomerates is very low).
- The fictitious particle cannot be an agglomerate, hence it is only sampled from the primary particle size distribution.

☞ Extension of the stochastic collision model

- The collision probability (based on a selected collision sphere of the agglomerate) predicts whether a collision occurs.
- The collision process is calculated in a coordinate system where the agglomerate is stationary.
- The point of impact on the surface of the selected collision sphere of the agglomerate is sampled stochastically

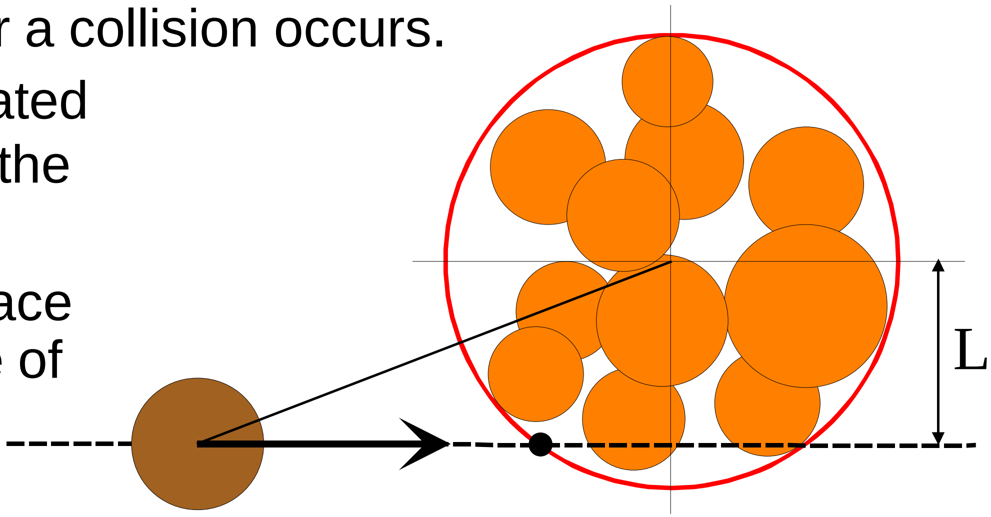

Agglomerate Structure Model 3

- A collision occurs if the lateral displacement *L* is smaller than the boundary trajectory Y_C (impact efficiency).
- Random rotation of the agglomerate in all three directions (since rotation is neglected).
- The particle collides with the primary particle in the agglomerate being closest to the impact point (tracking).
- Possible collision scenarios:

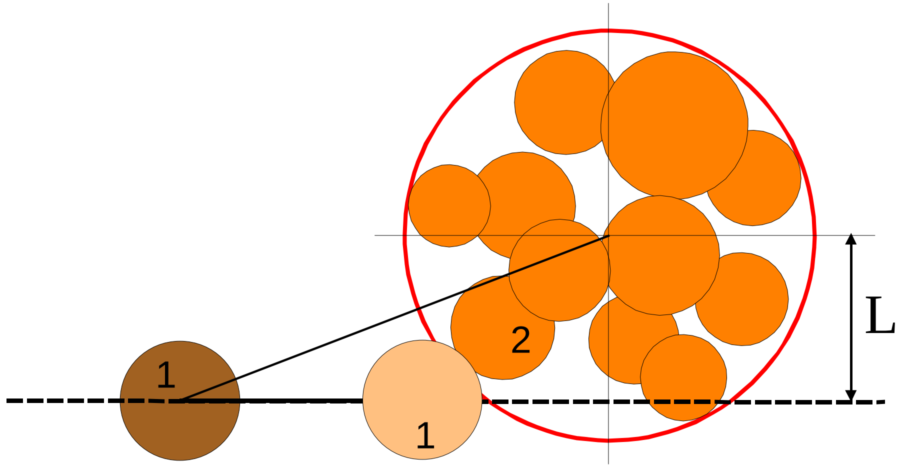

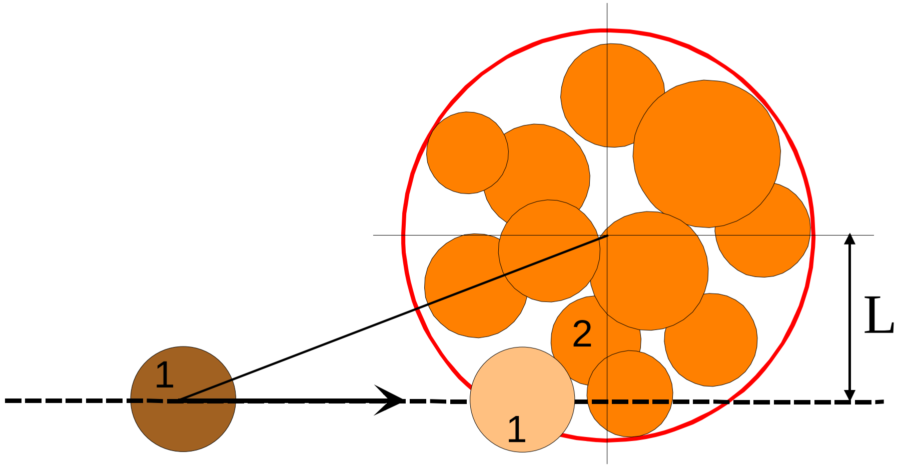

sticking

rebound

Viscous particles: penetration

Penetration Model for High Viscous Droplets

High viscous droplets penetrates into the low viscous droplet (spherical frame)

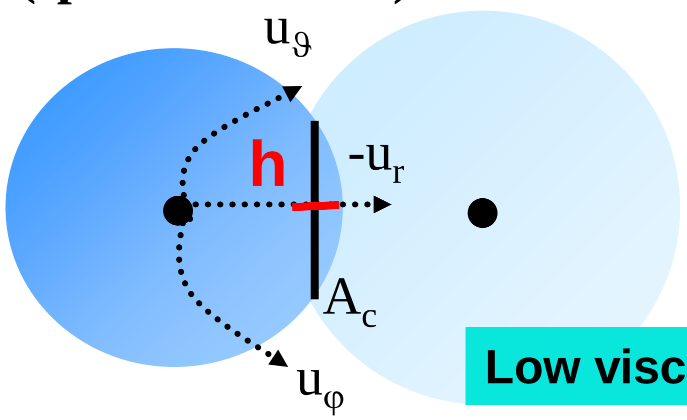

- Contact Area: $$d_{cont} = 2 \cdot \sqrt{h \cdot d_{Low} - h^2}$$

- Penetration depth: $$X_P = \frac{d_{High} + d_{Low}}{2} - r$$

$$h = X_P \quad \text{for} \quad r > 0$$

$$h = \frac{d_{Low}}{2} - r \quad \text{for} \quad r \le 0$$

Calculation of ***time-dependent penetration depth:***

Radial:

Motion of sphere in viscous liquid

$$m_{High} \cdot \frac{du_r}{dt} = -3 \cdot \pi \cdot \mu_{Low} \cdot d_{cont} \cdot u_r$$

$$\frac{dr}{dt} = u_r$$

Tangential:

Shear force across contact area

$$m_{High} \cdot \frac{du_\vartheta}{dt} = -\mu_{Low} \cdot d_{cont} \cdot u_\vartheta$$

$$\frac{d\vartheta}{dt} = \frac{u_\vartheta}{r}$$

Agglomeration Model for Solid Particles

- **The occurrence of agglomeration may be decided on the basis of an energy balance (dry particles → only Van der Waals forces):**

$$E_{k1} \le \Delta E_{vdw} + E_d$$

$$E_d = \left(1 - k_{pl}^2\right) E_{k1}$$

Ho and Sommerfeld (2002)

Van der Waals Energie:

$$\Delta E_{vdw} = -\int_{z_0}^{\infty} \frac{A}{6\,\pi\, z^3}\, \pi\, a^2\, dz$$

Restitution ratio:

$$k_{pl}^2 = \frac{E_{k1} - E_d}{E_{k1}}$$

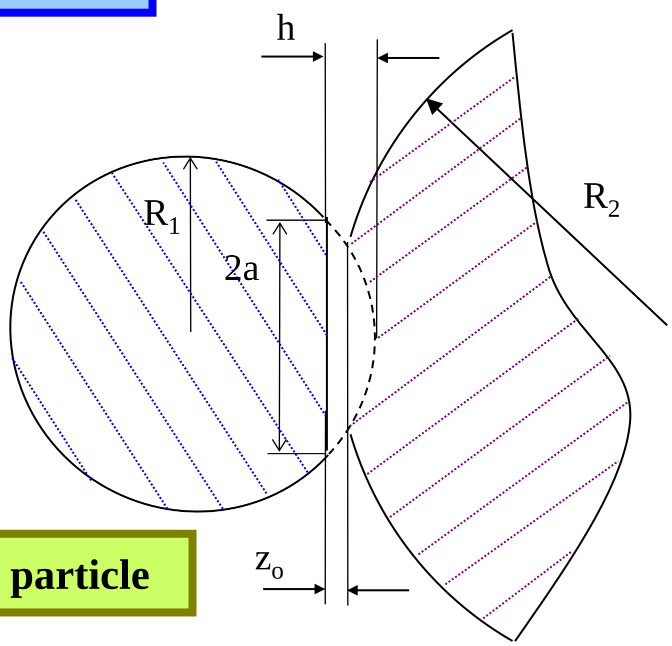

R1: smaller particle

- **Critical impact velocity:**

$$\left|\vec{U}_{kr}\right| = \frac{1}{2\,R_1}\, \frac{\left(1 - k_{pl}^2\right)^{1/2}}{k_{pl}^2}\, \frac{A}{\pi\, z_0^2\, \sqrt{6\, P_{pl}\, \rho_p}}$$

→

Agglomeration if:

$$\vec{U}_{rel} \cos\phi \le \left|\vec{U}_{kr}\right|$$

Geometry of the Spray Dryer 1

➲ **Geometry and operational conditions of spray dryer (NIRO Copenhagen):**

Dryer geometry:

H = 4096 mm

H_{cyl} = 1960 mm

D = 2700 mm

H_{out} = 3303 mm

D_{out} =210 mm

Annular Air Inlet

R_o = 527 mm

R_i = 447 mm

Air flow with swirl:

$\dot{m}_{air}$ = 1900 kg/h

ϕ_{air} = 1.1 mass-%

T_{air} = 452.5 K

U_{ax} = 9.8 m/s

U_{tan} = 2.4 m/s

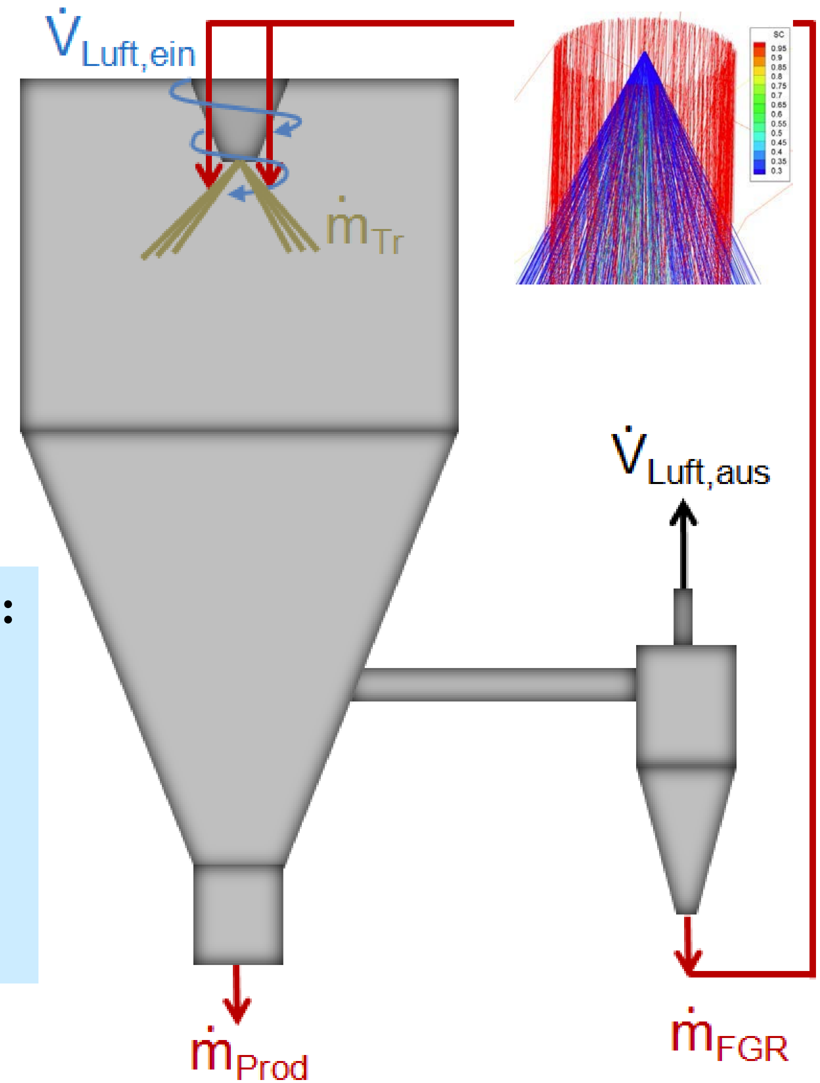

Fines return:

Annular inlet around the nozzle

D_o = 72 mm

D_i = 63 mm

U_{fine} = 37 m/s

ρ_{fine} = 440 kg/m³

Pressure nozzle:

Hollow cone nozzle

p_{nozzle} = 85 bar

Spray angle β = 52º

D_{nozzle} = 2 mm

H_{nozzle} = 270 mm

Maltodextrine DE-18

Solution: 29 mass-% solids

ρ_{drop} = 1090 kg/m^3

$\dot{m}_{solution}$ = 92 kg/h

$T_{solution}$ = 293 K

U_{av} = 127 m/s

Geometry of the Spray Dryer 2

➲ **Numerical discretisation and boundary conditions of the spray dryer:**

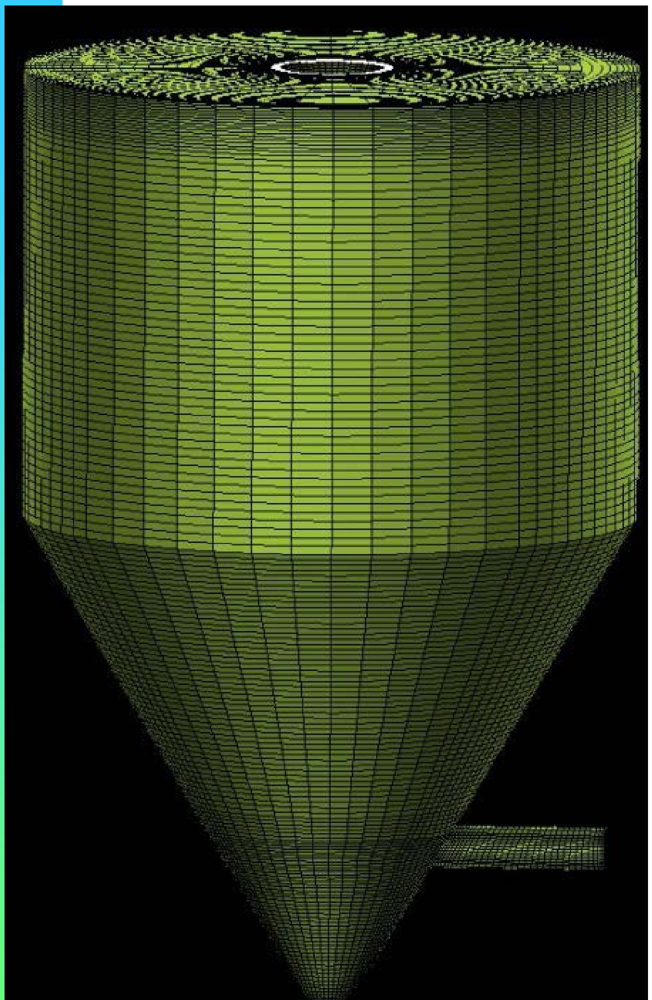

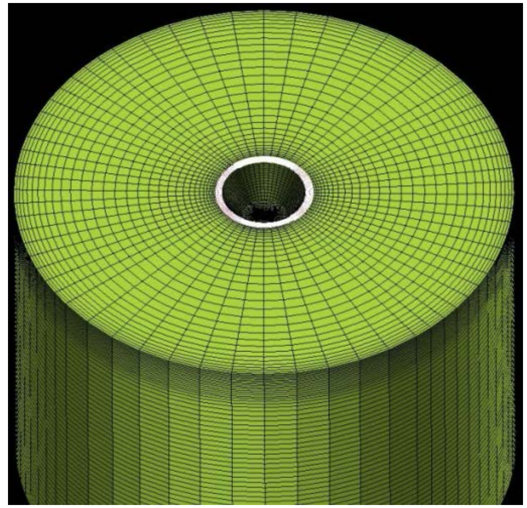

Discretisation:

138 blocks

586.564 meshes

Droplet and Particle Sizes

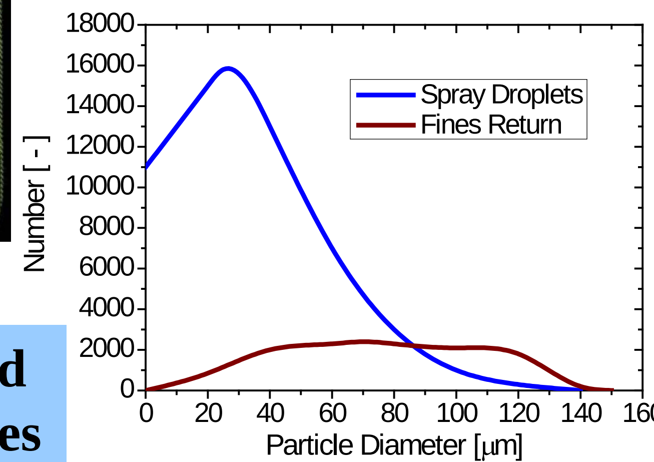

Inlet and boundary conditions:

Inlet: assumed velocity profiles

Walls: no-slip velocity

heat transfer coefficient ⇒ measurements

$h = 10.5\ W/(K\cdot m^2)$,

Outlet pipe: gradient free

Numerical Results Spray Dryer 1

☞ Calculated flow structure and temperature field in the dryer:

Velocity field

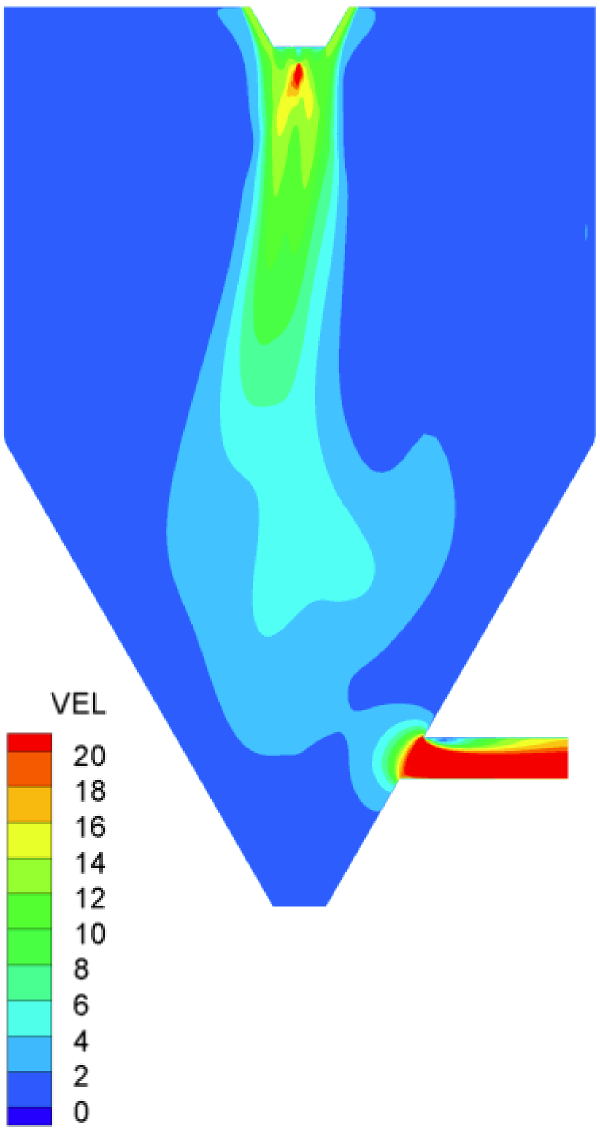

Water vapour concentration

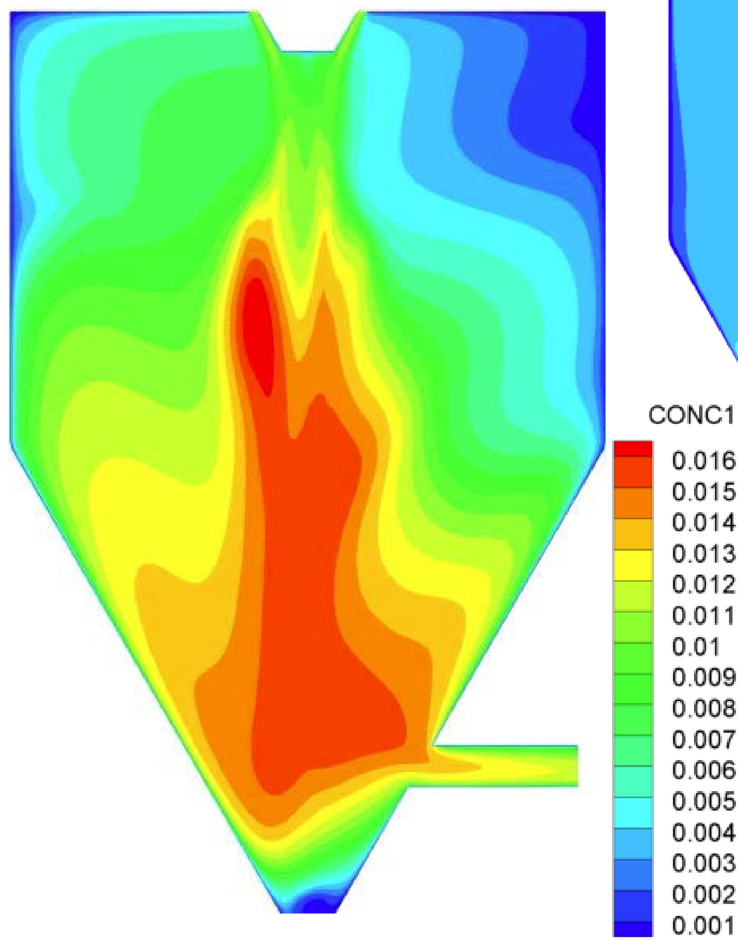

Temperature field

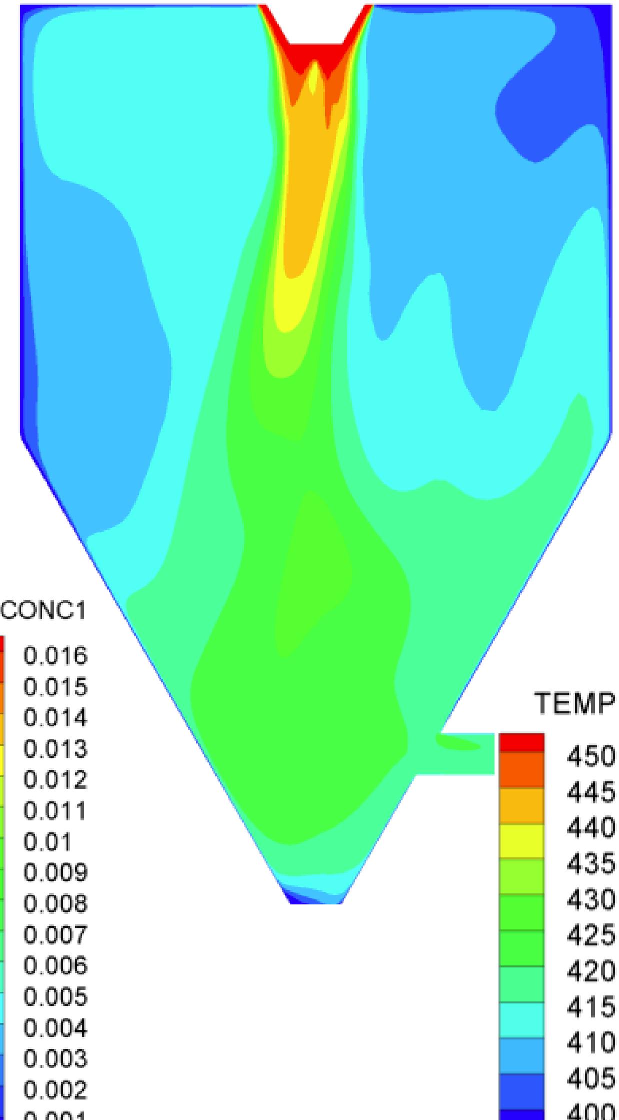

Numerical Results Spray Dryer 2

☞ **Particle phase properties throughout the spray dryer**

Particle trajectories

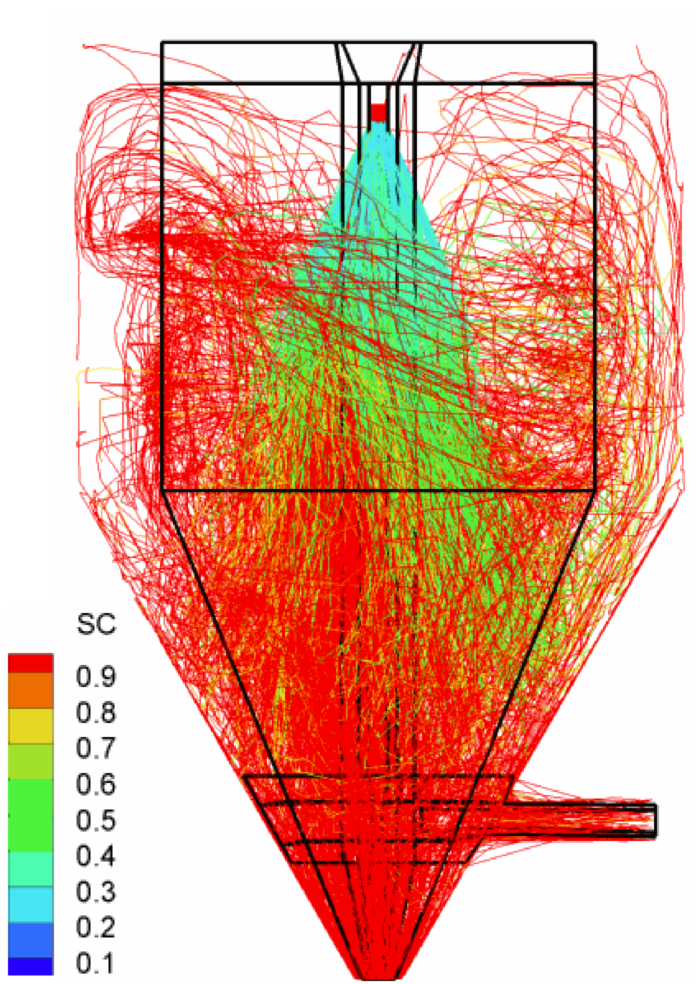

Particle concentration [kg/kg]

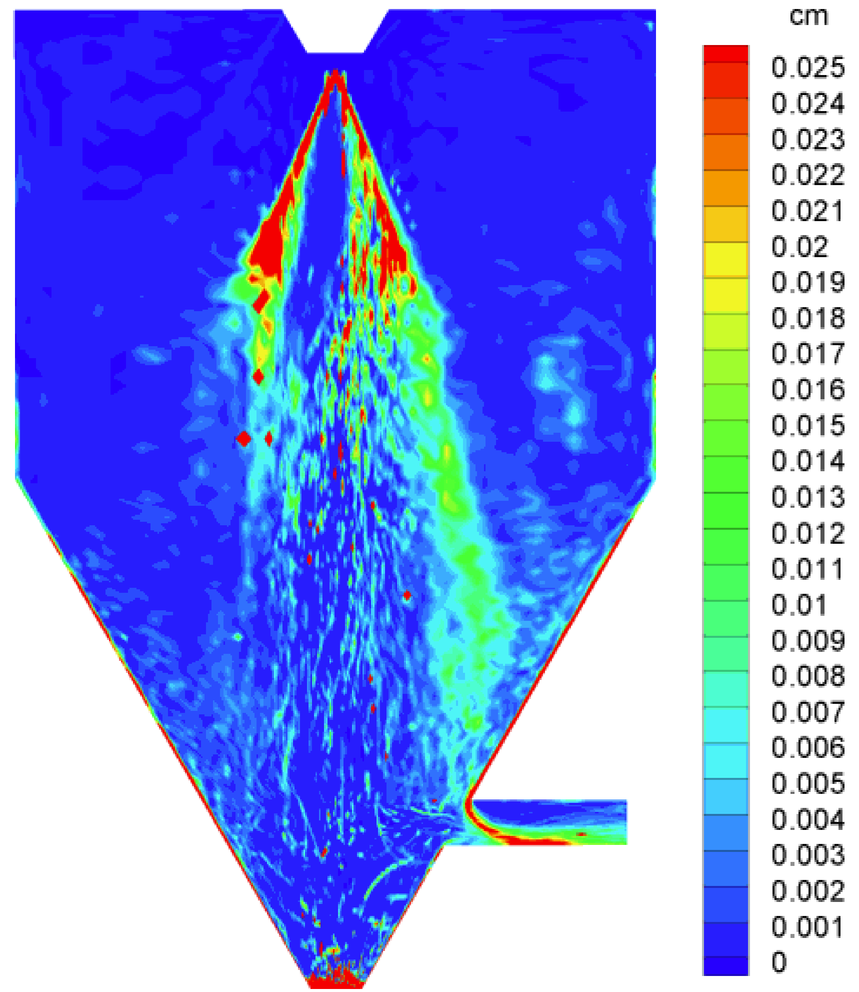

Numerical Results Spray Dryer 3

☞ **Particle-phase properties throughout the spray dryer**

Solids content in the particles

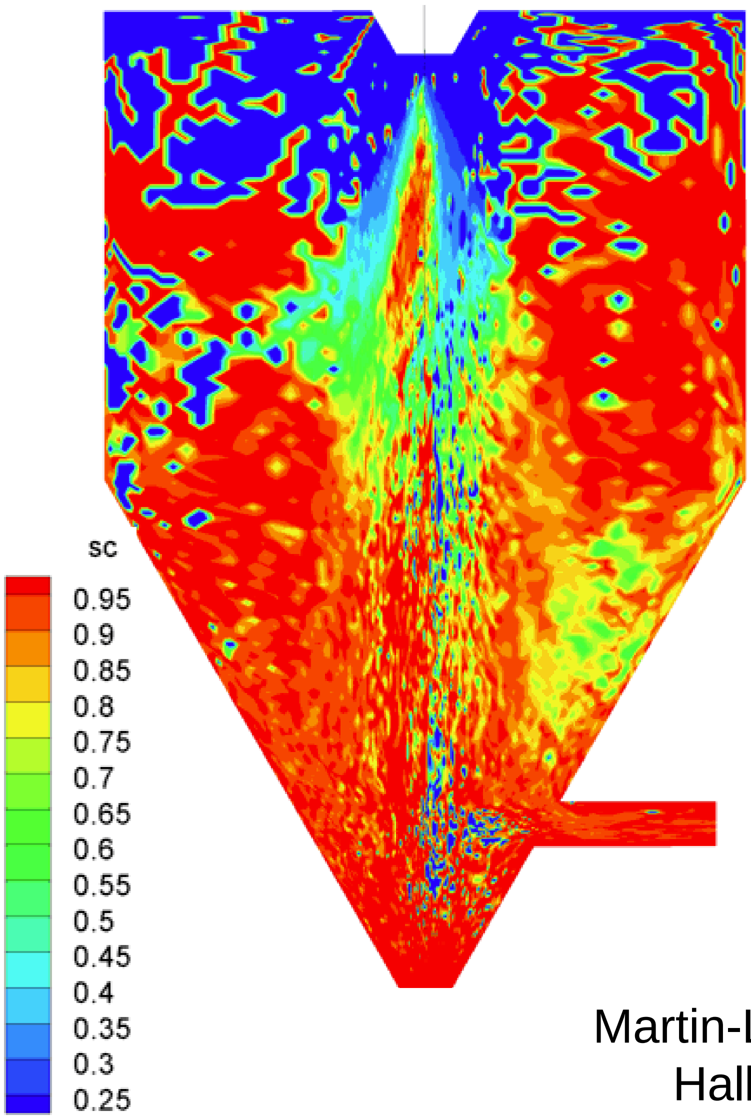

Local particle mean diameter

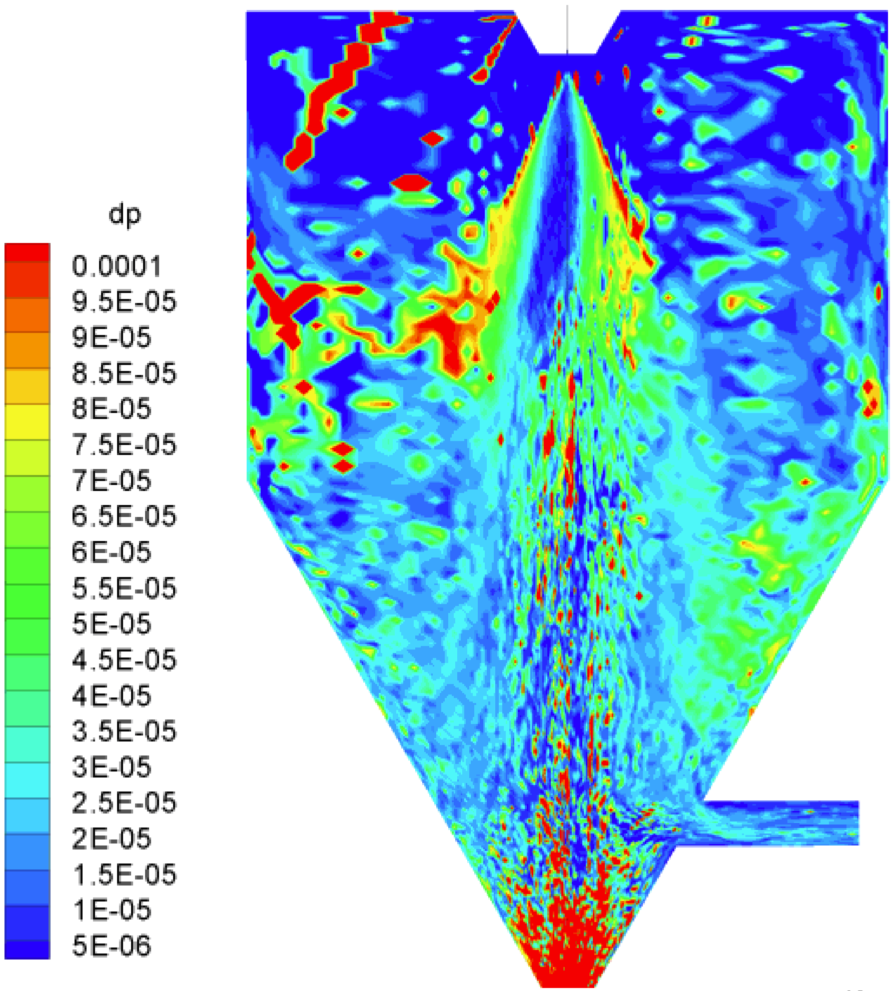

Numerical Results Spray Dryer 4

☞ **Properties of the agglomerates produced in the spray dryer**

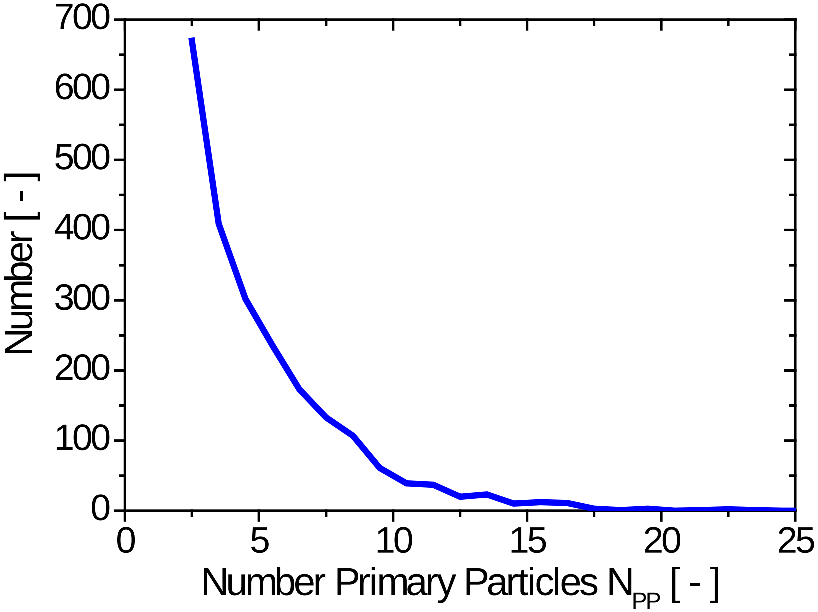

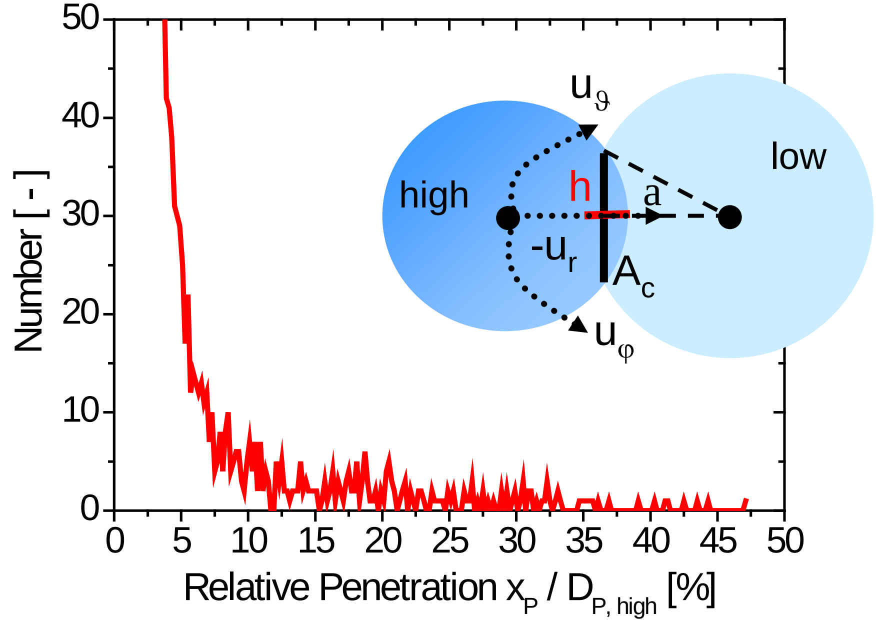

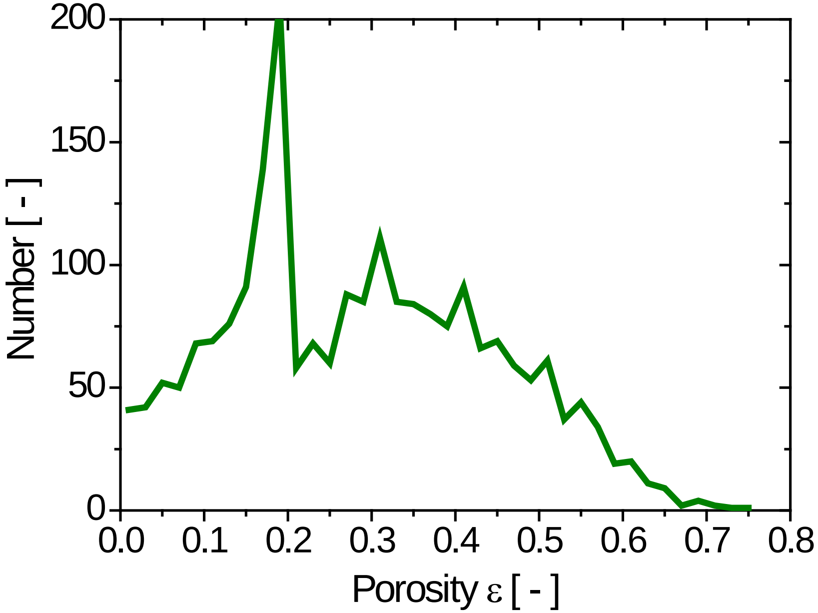

Porosity:

$$\varepsilon = 1 - \frac{V_{Part}}{V_{Hull}}$$

30 primary particles

$$\varepsilon_{hull} = 0.61$$

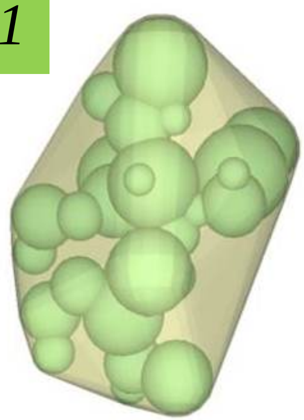

Numerical Results Spray Dryer 5

Simulated agglomerates compared with agglomerates collected from the spray dryer

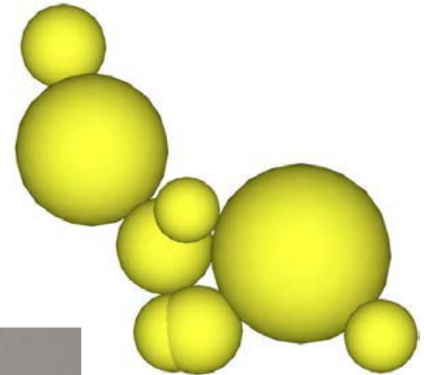

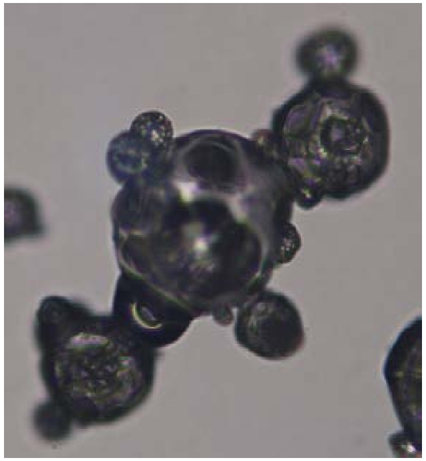

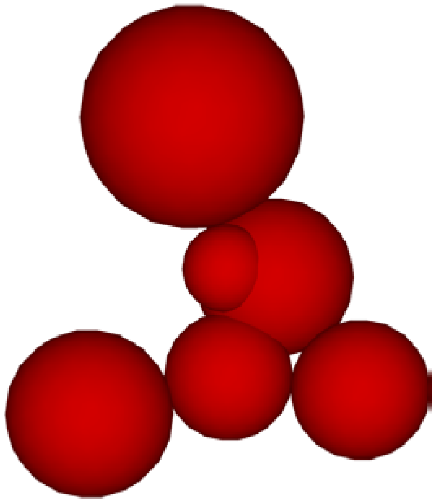

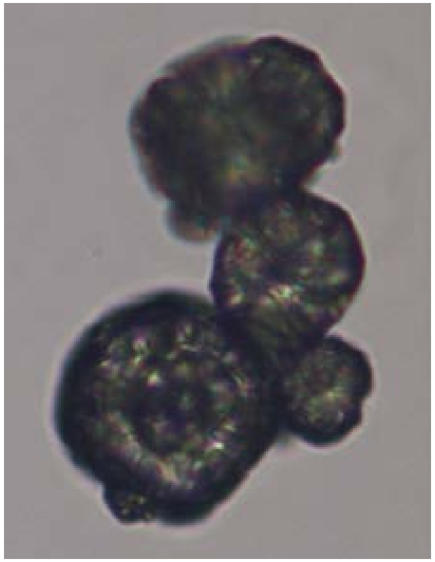

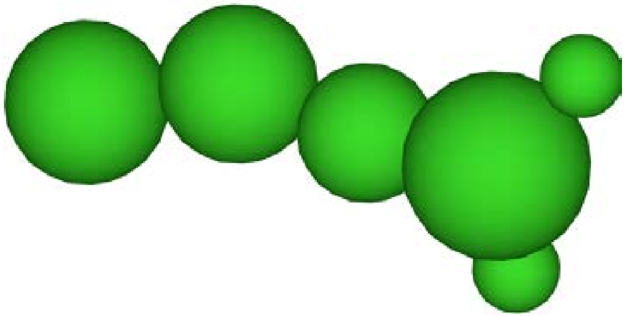

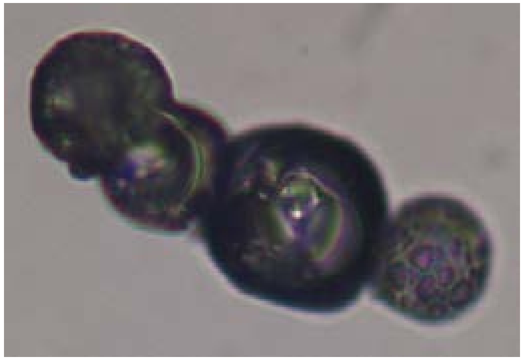

- **Sub-models for describing the behaviour of droplets and particles in a spray dryer have been developed and validated; i.e. drying, viscous droplet collisions and agglomeration model.**
- **The models will be jointly implemented in the in-house code FASTEST/Lag-3D and further validated.**
- **Extension of the droplet collision model for very high viscosities; i.e. up to several Pa·s.**

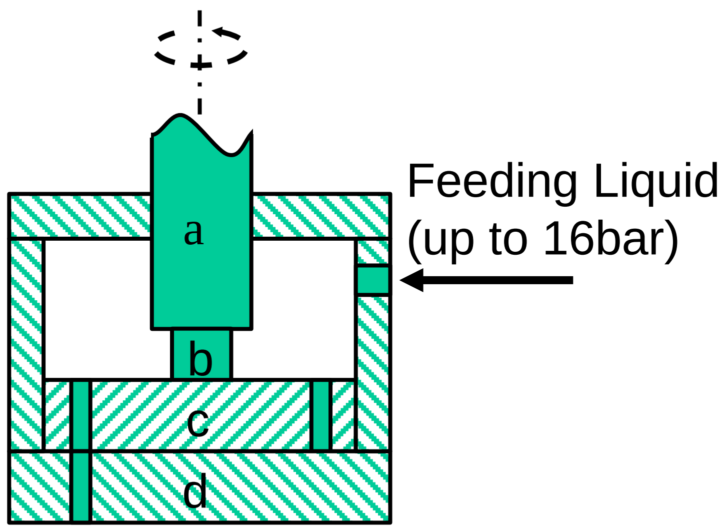

Outlet

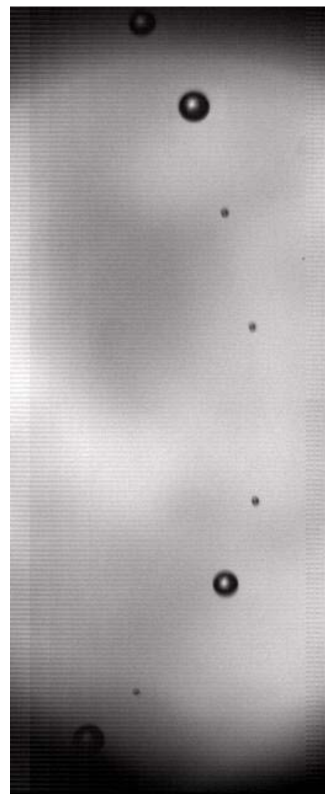

Coalescence

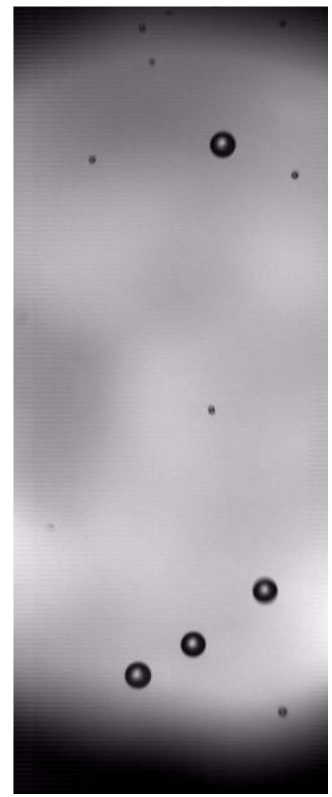

Stretching

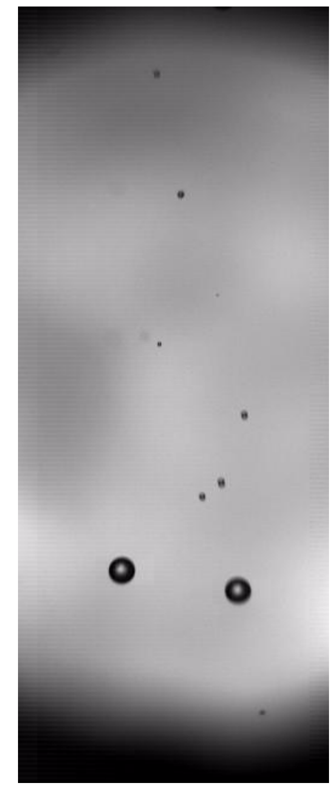

Separation

Outlook 2

- **Validation of the droplet collision models using a special laboratory spray dryer with interacting sprays.**

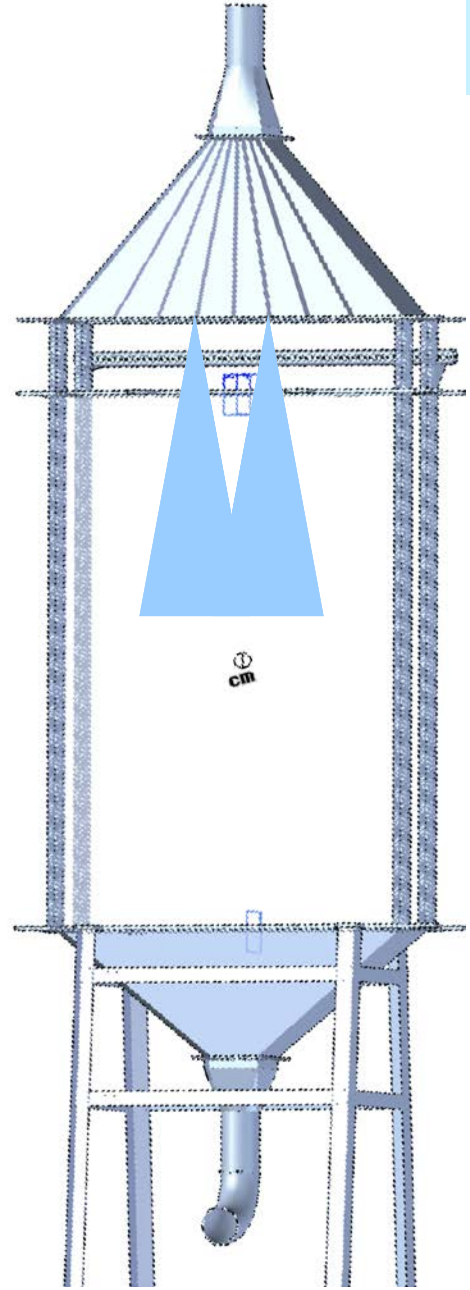

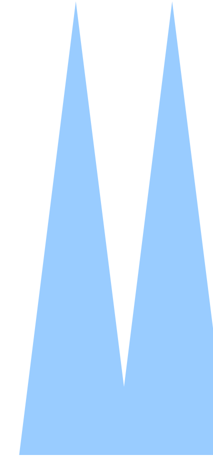

Acknowledgements

The financial support of projects by the Deutsche Forschungsgemeinschaft (DFG) is gratefully acknowledged.

The following Ph.D. students have contributed to the presented research:

Dipl.-Ing. Stefan Blei

M.Sc. Ali Darvan

M.Sc. Chi-Ahn Ho

Dipl.-Ing. Matthias Kuschel

Dr.-Ing. Hai Li

Dipl.-Ing. Sebastian Stübing

ANNOUNCEMENT

14th Workshop on Two-Phase Flow Predictions

07. – 10. September 2015

Zentrum für Ingenieurwissenschaften
Martin-Luther-Universität
Halle-Wittenberg
D-06099 Halle (Saale), Germany
www-mvt.iw.uni-halle.de

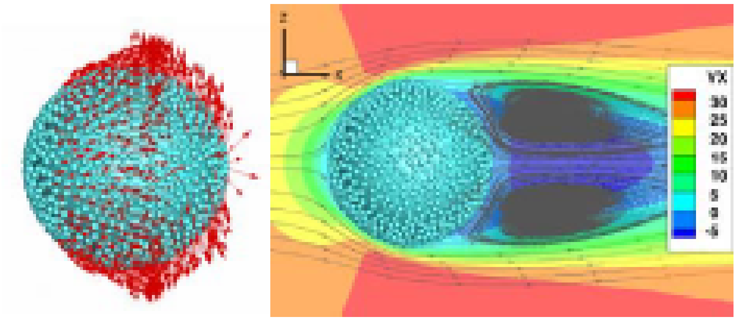

Lattice-Boltzmann Simulations: Flow about a particle coated with 882 drug particles at Re = 200, study related to drug particle detachment in an inhaler.